THE JOURNAL OF PHYSICAL CHEMISTRY A

Article

pubs.acs.org/JPCA

Quantum Mechanical Study of Sulfuric Acid Hydration: Atmospheric Implications

Berhane Temelso,[†] Thomas E. Morrell,[†] Robert M. Shields,[†] Marco A. Allodi,[†] Elena K. Wood,[†] Karl N. Kirschner,[‡] Thomas C. Castonguay,[§] Kaye A. Archer,[†] and George C. Shields*[,†]

[†]Dean's Office, College of Arts and Sciences, and Department of Chemistry, Bucknell University, Lewisburg, Pennsylvania 17837, United States

[‡]Department of Simulation Engineering, Fraunhofer-Institute for Algorithms and Scientific Computing (SCAI), Schloss Birlinghoven, 53754 Sankt Augustin, Germany

[§]Department of Chemistry, Iona College, New Rochelle, New York 10801, United States

Supporting Information

ABSTRACT: The role of the binary nucleation of sulfuric acid in aerosol formation and its implications for global warming is one of the fundamental unsettled questions in atmospheric chemistry. We have investigated the thermodynamics of sulfuric acid hydration using ab initio quantum mechanical methods. For $H_2SO_4(H_2O)_n$ where n = 1−6, we used a scheme combining molecular dynamics configurational sampling with high-level ab initio calculations to locate the global and many low lying local minima for each cluster size. For each isomer, we extrapolated the Møller−Plesset perturbation theory (MP2) energies to their complete basis set (CBS) limit and added finite temperature corrections within the rigid-rotor-harmonic-oscillator (RRHO) model using scaled harmonic vibrational frequencies. We found that ionic pair $(HSO_4^-{\cdot}H_3O^+)(H_2O)_{n-1}$ clusters are competitive with the neutral $(H_2SO_4)(H_2O)_n$ clusters for $n \geq 3$ and are more stable than neutral clusters for $n \geq 4$ depending on the temperature. The Boltzmann averaged Gibbs free energies for the formation of $H_2SO_4(H_2O)_n$ clusters are favorable in colder regions of the troposphere (T = 216.65−273.15 K) for n = 1−6, but the formation of clusters with $n \geq 5$ is not favorable at higher (T > 273.15 K) temperatures. Our results suggest the critical cluster of a binary H_2SO_4−H_2O system must contain more than one H_2SO_4 and are in concert with recent findings[1] that the role of binary nucleation is small at ambient conditions, but significant at colder regions of the troposphere. Overall, the results support the idea that binary nucleation of sulfuric acid and water cannot account for nucleation of sulfuric acid in the lower troposphere.

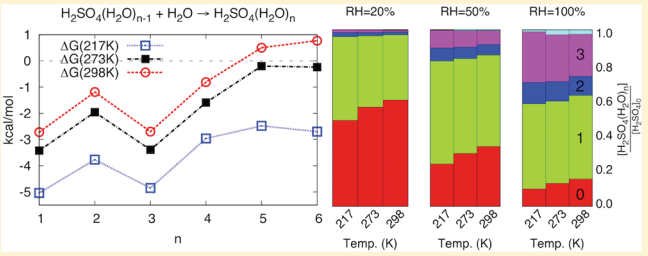

1. INTRODUCTION

In the atmospheric sciences, the term aerosol refers to any particulate matter suspended in a gas. Primary aerosols are released directly into the atmosphere from both natural and anthropogenic sources, whereas secondary aerosols form in the atmosphere through different physical and chemical means. Atmospheric aerosols have a significant net cooling effect on the global climate, but the effect's extent is uncertain.[2] Aerosols exert both a direct and an indirect effect on the climate. Depending on their composition (sulfates, nitrates, soot, salts, etc.), they directly scatter and absorb radiation differently; the scattering of incoming radiation causes atmospheric cooling, whereas absorption results in atmospheric warming. The first indirect effect is caused through the subset of the aerosol population called cloud condensation nuclei (CCN). A larger number of these nuclei increases the cloud albedo (reflectivity) effect and reduces the amount of radiation reaching the earth's surface. A second indirect effect is the reduced precipitation efficiency and increased lifetime of the cloud. Even though our understanding of the effect of aerosols on the earth's climate has improved substantially over the past decade, it remains the most uncertain parameter in atmospheric studies of global warming.[2−5]

Of the many aerosol species, sulfates have the largest direct effect amounting to -0.4 ± 0.2 W m^{-2} on the global radiation balance.[6] The main source of sulfates in the atmosphere is SO_2 emitted from fossil fuel and biomass burning. SO_2 is readily oxidized by the hydroxyl radical (OH) to form SO_3, which reacts with water vapor to produce H_2SO_4. Gas-phase sulfuric acid has a low vapor pressure and it gets supersaturated very easily. As a result, it undergoes a quick transition from gas to condensed phase and serves as an effective nucleating species for water vapor and other compounds.[5] Experimental observations have shown that new particle formation in the atmosphere depends on the concentration of sulfuric acid in all kinds of environments ranging from urban areas to pristine

Received: December 10, 2011
Revised: January 31, 2012
Published: February 1, 2012

ACS Publications © 2012 American Chemical Society

forests, the marine to continental boundary layer, and the lower to free troposphere.[7−11] The growth of subnanometer molecular clusters to aerosols ranging from 3 to 50 nm is thought to occur through different nucleation processes depending on the atmospheric conditions.[12] Binary homogeneous nucleation (BHN) of water−sulfuric acid nucleation is expected to play a role in the cold free troposphere and environments that are rich in H_2SO_4 precursor gases (SO_2/SO_3) such as combustion engines and volcanic or industrial plumes. In the continental boundary layer, ternary homogeneous water−sulfuric acid−ammonia nucleation (THN),[13] or one involving amines[14,15] and organic acids[16,17] is expected to be significant. Ion-induced nucleation has been implicated as another process that can explain experimentally observed new particle formation rates.[18−20] Recent studies suggest that small particles less than 3 nm in diameter initiate aerosol formation.[8] Unfortunately, the size detection of the experimental apparatus has been limited to 3 nm or larger in diameter until recent advances extended it to 1.3−1.5 nm.[8,21,22] The challenge of detecting, counting, and determining the exact composition of these molecular clusters as they grow to a critical cluster has hindered the development of models of aerosol activation and growth based on experiment. The recent Cosmics Leaving OUtdoor Droplets (CLOUD) experiment allowed scientific insight on some questions about the mechanism of sulfuric acid aerosol formation and the role that ternary nucleation and galactic cosmic rays play in the process.[1]

As previously mentioned, sulfuric acid is very hygroscopic and the aerosols it forms grow large enough to serve as important CCNs. Berndt et al.[23] showed that a concentration of $\sim 10^7$ H_2SO_4 molecules per cubic centimeter (molecules·cm^{-3}) is sufficient to observe aerosol formation. In the laboratory, they showed that gas-phase particle formation starting from a liquid reservoir required sulfuric acid concentrations of 10^{10} molecules·cm^{-3}, whereas in situ gas-phase formation of H_2SO_4 in a flow tube required only 10^7 molecules·cm^{-3} for particle formation. An amount of 10^5−10^8 molecules·cm^{-3} corresponds to typical atmospheric sulfuric acid concentrations. Nucleation of H_2SO_4−H_2O has been explored using theoretical methods.[24−55] Most of the theories use a version of classical nucleation theory (CNT) and thus share the use of bulk properties, such as surface tension, molar volume, partial molar volumes, vapor pressures, and equilibrium vapor pressures. A useful comparison of CNT and kinetic models[56,57] has been provided by Mirabel's research group for binary homogeneous nucleation in the H_2SO_4−H_2O system.[58] They conclude that for slow nucleation rates (less than 10^3 cm^{-3} s^{-1}), their kinetic model corresponds exactly to the CNT model of Shugard, Heist, and Reiss.[28] However, for nucleation rates exceeding 10^3 cm^{-3} s^{-1}, up to 30% of the nucleation flux results from cluster−cluster collisions that are not considered in CNT. Nevertheless, a large discrepancy between predicted and observed nucleation rates exists. The dependence of the nucleation rate (J) on the concentration of sulfuric acid ($J \propto K[H_2SO_4]^n$) is predicted to be steep ($n > 2$) according to kinetic models and CNT,[56,58] whereas atmospheric observations indicate that $n = 1$, 2.[7,11,21]

Because current models of secondary aerosol formation largely underestimate what is observed in the atmosphere,[59] we intend to try and understand this discrepancy using accurate thermodynamic values for the initial stages of sulfuric acid/water cluster formation.[7] Experiments reveal that even at low (<20%) relative humidity, most sulfuric acid molecules form hydrates.[60,61] The formation of hydrates decreases the number of free acid monomers, stabilizes the vapor, and increases the nucleation barrier substantially enough to reduce the CNT nucleation rates by a factor of 10^3−10^8 compared to what they would be in the absence of hydration.[48,61] However, Bein and Wexler[55] argue that better agreement between experimental and theoretical nucleation rates is found when the total sulfuric acid concentration includes both the acid monomer and the acid hydrates. Predictions of hydration are sensitive to the thermodynamics of hydrate formation. Jaecker-Voirol and Mirabel[31,32,62] have extended the capillary liquid drop (CLD) model, which uses bulk free energy and surface tension of macroscopic liquid droplets, to obtain equilibrium constants for sulfuric acid hydrate formation,[31,32,62] but this method's validity has been questioned.[61] Experiments have shown that CLD overestimates the extent of hydration and highlights the need for accurate thermodynamics of hydrate formation in small molecular clusters.[60,61] To incorporate the effect of hydration on nucleation rates, many models have used a combination of experimental[63] and theoretical equilibrium constants of hydration.[48,64] The error bars on the experimental equilibrium constants[63] are large, and the computed values vary substantially among DFT[65−72] and ab initio methods.[73,74] The most reliable study of sulfuric acid hydrate formation to date was published by Kurtén et al.,[74] who have shown that MP2 ab initio calculations extrapolated to the complete basis set limit and corrected for vibrational anharmonicity yielded equilibrium constants of hydration that are close to the available experimental values of Hanson and Eisele.[63] The work presented here extends their results by (a) employing a more robust basis set extrapolation scheme, (b) rigorously accounting for molecular symmetry in the calculation of finite temperature corrections, (c) including the study of pentahydrates and hexahydrates, (d) sampling a larger number of hydrate isomers, (e) incorporating the contribution of all low-lying isomers via Boltzmann averaging, and (f) including a discussion of the most recent experimental results on the sulfuric acid−water system. After searching for the minimum energy structures of sulfuric acid hydrates $H_2SO_4(H_2O)_{n=1-6}$, we determined the thermodynamic properties of these different clusters and used the computed Gibbs free energies to estimate the concentrations of these hydrates at three conditions germane to the troposphere. The results of this work provide insight into the binary nucleation of sulfuric acid and water, and this work is a continuation of our long-standing efforts to explore cluster formation of water, and to better understand atmospheric processes.[75−95]

2. METHODOLOGY

Our initial structures for $H_2SO_4(H_2O)_{n=1-3}$ include those reported by Kurtén et al.[74] as well as other low energy isomers we identified. We report structures and thermodynamic properties of three isomers for $n = 1$, three isomers for $n = 2$, and five isomers for $n = 3$. For $H_2SO_4(H_2O)_{n=4-6}$, we used a molecular dynamics (MD) sampling scheme that has previously been applied to water clusters[81,93−95] and other hydrates.[87,90,92] In this two-step gas-phase MD simulation using the AMBER 9 package,[96] the system was first heated from 5 K to the final temperature T_f over a period of 1 ns. In the second step, the temperature remained at T_f for a 10 ns production run. Simulations were repeated at various final temperatures until reaching a temperature where the cluster dissociates; we then used the temperature that was slightly lower than the dissociation temperature to ensure a full 10 ns run. This T_f

was 95, 95, and 105 K for n = 4, 5, and 6, respectively. All MD simulations were performed with a nonbonded cutoff of 20 Å and weighting factors of 2.0 and 1.2 for the nonbonded and electrostatic interactions. Our preliminary results suggested that the TIP4P water model replicates MP2 geometries of water clusters well, a finding verified by a recent publication,[97] so we used the TIP4P water model along with the generalized AMBER force field (GAFF).[98] From these simulations we extracted 200 configurational "snapshots" of the clusters at even intervals using the ptraj module. These snapshots were used as starting structures for MP2/6-31G* geometry optimizations using Gaussian 09.[99] All configurations that converged after 200 optimization cycles were sorted by their MP2/aug-cc-pVDZ//MP2/6-31G* energies and those within 7 kcal mol^{-1} of the global minimum were subject to an RI-MP2/aug-cc-pVDZ optimizations using the ORCA 2.8.0 package.[100]

We used the frozen-core resolution-of-the-identity MP2 (RI-MP2) method[101,102] with Dunning's augmented correlation-consistent basis sets (aug-cc-pVNZ, N = D, T, Q)[103−105] and corresponding auxiliary basis sets[106] to obtain RI-MP2/CBS binding energies. We denote Dunning's aug-cc-pV*N*Z basis sets by aVNZ for the sake of brevity. All structures were fully optimized at the RI-MP2/aVDZ level using analytic gradients[107] with strict convergence criteria ($\Delta E < 1 \times 10^{-6}$ au; rms gradient $<3 \times 10^{-5}$ au/Å and rms displacement $<6 \times 10^{-4}$ Å). Our investigation of the sensitivity of binding energies to geometries computed using RI-MP2/aVDZ and RI-MP2/aVTZ showed that the difference between the two is very small (Table S1, Supporting Information). Also, we have evaluated the importance of using a basis set with a tight d-function such as aug-cc-pV(N+d)Z basis sets.[108] The extra d-function turns out to have little effect on geometry, energy, and vibrational frequencies of $H_2SO_4(H_2O)_n$, as shown in Table S2, Supporting Information.

Computing interaction energies of noncovalently bonded systems using MP2 with a finite basis is plagued by basis set superposition errors (BSSE) on top of basis set incompleteness errors (BSIE). One can address the two issues by extrapolating the energy to the complete basis set (CBS)[109] limit and employing counterpoise (CP)[110] corrections. The RI-MP2 CBS limit is estimated using two extrapolation schemes. Halkier et al.[111,112] recommend the extrapolation of the SCF energy using an exponential function and the RI-MP2 correlation energy using an inverse cubic function:

$$E_{\mathrm{CBS}}^{\mathrm{SCF}} = E_N^{\mathrm{SCF}} + B\mathrm{e}^{-\mathrm{AN}}$$

$$E_{\mathrm{CBS}}^{\mathrm{corr}} = \frac{N^3 E_N^{\mathrm{corr}} - (N-1)^3 E_{N-1}^{\mathrm{corr}}}{N^3 - (N-1)^3}$$

$$E_{\mathrm{CBS}}^{\mathrm{RI\text{-}MP2}} = E_{\mathrm{CBS}}^{\mathrm{SCF}} + E_{\mathrm{CBS}}^{\mathrm{corr}} \qquad (1)$$

Here A and B are fitting parameters $E_{\mathrm{CBS}}^{\mathrm{SCF}}$, $E_{\mathrm{CBS}}^{\mathrm{corr}}$, and $E_{\mathrm{CBS}}^{\mathrm{RI\text{-}MP2}}$ are the complete basis set SCF, RI-MP2 correlation, and total energies. We use the aug-cc-pVNZ (N = D, T, Q) for the SCF and aug-cc-pVNZ (N = T, Q) basis sets for the correlation energy extrapolations. Alternatively, the 4-5 inverse polynomial scheme[113,114] extrapolates the total energy as

$$E_{\mathrm{N}}^{\mathrm{RI\text{-}MP2}} = E_{\mathrm{CBS}}^{\mathrm{RI\text{-}MP2}} + \frac{b}{(N+1)^4} + \frac{c}{(N+1)^5} \qquad (2)$$

where $E_{\mathrm{N}}^{\mathrm{RI\text{-}MP2}}$ is the RI-MP2/aVNZ//RI-MP2/aVDZ energy, $E_{\mathrm{CBS}}^{\mathrm{RI\text{-}MP2}}$ is the extrapolated RI-MP2/CBS energy, and N is the largest angular momentum number for the aVNZ basis set. The 4-5 inverse polynominal scheme has been used extensively for water clusters.[93,95,115−118] The performance of the two extrapolation schemes is judged by comparison with benchmark values from the explicitly correlated DF-MP2-F12[119] method implemented in Molpro.[120] We used the DF-MP2-F12 method employing the 3C(FIX) ansatz[121] with cc-pVQZ-F12 (VQZ-F12) orbital basis,[122] the recommended aVQZ/MP2fit density fitting basis, and the VQZ/JKfit auxiliary basis for the F12 part. The binding energies from our DF-MP2-F12/VQZ-F12 calculations are essentially at the basis set limit, as recent works have shown.[123,124] We also studied the convergence of the counterpoise (CP) corrected and uncorrected binding energies to determine which scheme leads to a faster convergence of the binding energy to basis set limit.

We chose not to include higher-order electron correlation corrections using MP4, CC2, or CCSD(T) because the additivity of these corrections has been shown to be unreliable for hydrogen bonded systems even though it works well for other noncovalently bonded systems.[125] For small water clusters, Xantheas[116,126] and Klopper et al.[127] concluded that a CCSD(T) correction to the MP2 binding energy is small and it is often canceled out by core−valence correlation corrections that are not included in frozen-core MP2 calculations like ours.

Zero-point corrected energies $[E(0)]$, energies including finite temperature corrections $[E(T)]$, enthalpies $[H(T)]$, and Gibbs free energies $[G(T)]$ for a standard state of 1 atm were calculated by combining the RI-MP2/aVDZ thermodynamic corrections with the RI-MP2/CBS electronic energies. Harmonic vibrational frequencies were computed numerically at the RI-MP2/aVDZ level using central differences with step sizes of 0.005 Å. Thermodynamic corrections are traditionally calculated from canonical partition functions with the assumption that the translational, rotational, and vibrational degrees of freedom can be sufficiently treated in the framework of ideal gas, rigid rotor, and harmonic oscillator (RRHO) approximations. The harmonic approximation of vibrational modes is particularly problematic in the case of low frequency, large amplitude, intermolecular modes of weakly bound systems like our molecular clusters. We have partially corrected for the deviation from harmonic behavior by scaling the harmonic vibrational frequencies to match second-order vibrational perturbation theory (VPT2)[128] anharmonic ones. For small water clusters, we have previously determined and applied multiplicative scaling factors for the ZPVE, and the frequencies input into $\Delta H_{\mathrm{vib}}(T)$ and $S_{\mathrm{vib}}(T)$ expressions specifically for water clusters using MP2/aVDZ.[94,95,129] Following that same procedure, we calculated VPT2/MP2/aVDZ fundamental frequencies for three $H_2SO_4(H_2O)$ and three $H_2SO_4(H_2O)_2$ isomers using Gaussian 09[99] with tight convergence criteria and small displacements (0.001 Å) used in the numerical calculation for cubic and semidiagonal quartic force constants. We then determined the optimal scaling factors for $(H_2SO_4)(H_2O)_n$ clusters, and the ZPVE, ΔH_{vib}(216.65 K), S_{vib}(216.65 K), ΔH_{vib}(273.15 K), S_{vib}(273.15 K), ΔH_{vib}(298.15 K), and S_{vib}(298.15 K) scaling factors are 0.979, 1.101, 1.123, 1.083, 1.108, 1.077, and 1.102, respectively (the harmonic and VPT2 fundamental frequencies are included in Tables S4−S7, Supporting Information).

Because of the small energetic differences, we have reported the numbers to the second decimal place to preserve first place information; the error bars in this method are expected to be on the order of many tenths of a kcal mol^{-1}. The presence of

many stable structures within available thermal energy (k_bT) suggests that a meaningful free energy for a cluster of size n must include a weighted account of all isomers of $H_2SO_4(H_2O)_n$. We weight the contribution of each low energy isomer by its Boltzmann factor to get the Boltzmann averaged enthalpies and free energies as described in the Supporting Information. The Boltzmann averaged free energies are combined with realistic estimates of concentrations of sulfuric acid and water vapor in the troposphere to estimate the abundance of sulfuric acid hydrates at equilibrium. Molecular graphics were generated using Chimera 1.5 and its default hydrogen bond definitions.[130] Standard state conditions are 1 atm pressure and the stated temperature.

3. RESULTS

The $H_2SO_4(H_2O)_{n=1,2}$ isomers are used to validate important elements of our methodology. For example, Figure 1 shows that

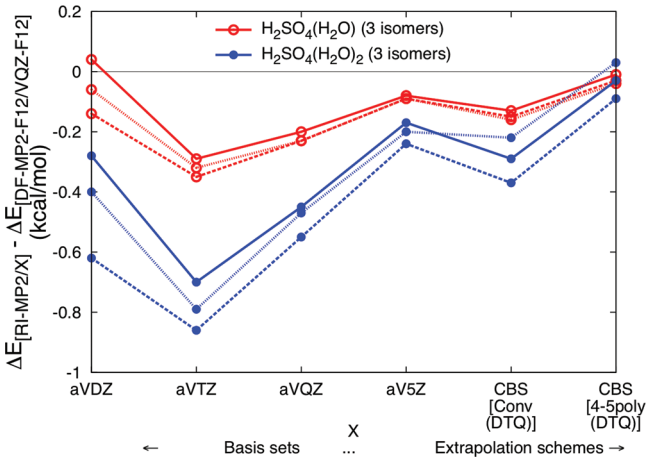

Figure 1. Difference between the RI-MP2/X and DF-MP2-F12/VQZ-F12 binding energy for six isomers of $H_2SO_4(H_2O)_{n=1,2}$, where X represents different basis sets and extrapolation procedures.

convergence of the binding energy is nonmonotonic and that one must include at least the aVQZ basis set to properly extrapolate to the basis set limit. Relying on the aVDZ-aVTZ extrapolation would give binding energies that are too low. Figure 1 also demonstrates that the conventional Halkier extrapolation using the aVNZ (N = D, T, Q) basis gives RI-MP2 binding energies that are lower than that from DF-MP2-F12/VQZ-F12, whereas the 4-5 inverse polynomial scheme match the benchmark values very closely. Thus, for this system, the 4-5 inverse polynomial scheme is better than the conventional basis set extrapolation. Figure 2 illustrates that the counterpoise corrected and uncorrected binding energies converge to the same limit when extrapolated using the 4-5 inverse polynomial scheme, whereas employing the Halkier scheme leads to slightly different limits. This further validates the use of the 4-5 inverse polynomial extrapolation. Aside from basis set extrapolation, correcting for vibrational anharmonicity is necessary to achieve accurate thermodynamic information.

Table 1 and Figure 3 illustrate that scaling factors developed by comparing the harmonic and VPT2 anharmonic ZPVE and $\Delta H_{vib}(T)$ and $S_{vib}(T)$ of $H_2SO_4(H_2O)_{n=1,2}$ effectively map the harmonic quantities to their anharmonic analogs. Applying the scaling factors derived from $H_2SO_4(H_2O)_{n=1,2}$ to all the larger clusters reveals that the anharmonic corrections typically lower the $\Delta G(298.15\ K)$ of adding a water monomer to an existing hydrate by about 0.4 kcal mol^{-1}. However, it does not change the relative conformational energy of isomers significantly.

The 63 minima reported in this study for $H_2SO_4(H_2O)_{n=1-6}$ are shown in Figures 4−9 in order of increasing electronic energy. To keep the size manageable, we only show those isomers whose relative electronic energy ($\Delta\Delta E$) or standard state Gibbs free energy [$\Delta\Delta G(298.15\ K)$] are within 4 kcal mol^{-1} of the global minimum isomer. The scaled harmonic RI-MP2/CBS binding energies for all the clusters are reported in Tables 2−5. Aside from $H_2SO_4(H_2O)_{n=1,2,6}$, the electronic energy (E_e) and $\Delta G(298.15\ K)$ global minima are different for the bigger clusters. The stability of the clusters varies on the basis of (a) the cis/trans configuration of H_2SO_4, (b) the dissociation of $H_2SO_4(H_2O)_n$ into ionic pairs, (c) the number of hydrogen bonds, (d) the type of hydrogen bonds, and (e) the quasi-planar or 3-D nature of the hydrogen bond network. The interplay between these factors determines which isomers are predominantly present at a certain temperature. All of the stable structures form closed hydrogen bond rings. Both acidic hydrogens of the sulfuric acid are hydrogen bonded in the vast majority of the low energy isomers for $n > 1$. The quasi-planar clusters typically have higher entropy (hence a lower free energy) than the more cage-like clusters. As a result, the $\Delta G(298.15\ K)$ global minima for $H_2SO_4(H_2O)_{n=1-3}$ all have quasi-planar structures. For $H_2SO_4(H_2O)_{n=4,5}$, cage-like ionic pair clusters are the most stable in terms of enthalpy, but the quasi-planar neutral clusters have lower free energies at 298.15 K. For $n = 6$, an ionic pair cluster is the most stable isomer at least until $T = 298.15$ K.

The effect of Boltzmann averaging is shown to be relatively small in Figure 10. The Boltzmann averaged scaled harmonic RI-MP2/CBS binding energies are reported in Table 6 and graphed in Figure 11. The growth of $H_2SO_4(H_2O)_{n=1-6}$ is thermodynamically favorable at $T = 216.65$−273.15 K, but only $n = 1$−4 are likely to form at $T = 298.15$ K in a closed binary system of H_2SO_4 and H_2O. At $T > 273.15$ K, the enthalpic stabilization provided by the ionic pair formation [$H_2SO_4(H_2O)_{n=5,6} \rightarrow HSO_4^-(H_3O^+)(H_2O)_{n=4,5}$] is not enough to overcome the entropic penalty of forming compact three-dimensional structures. As a result, the $\Delta G(298.15\ K)$ for the addition of a water to $H_2SO_4(H_2O)_{n>4}$ is positive.

We have predicted the abundance of sulfuric acid hydrates in a closed system containing sulfuric acid and water vapor by using our Boltzmann averaged Gibbs free energies and the ambient partial pressures of sulfuric acid and water. Simultaneously solving a set of mass-balance equations reveals that for the conditions of $T = 216.65$, 273.15, and 298.15 K, RH = 20%, 50%, 100%, and $[H_2SO_4]_0 = 5 \times 10^7$ cm^{-3}, the abundance of different hydrates depends significantly on the temperature and relative humidity. Under these conditions, 10−60% of the sulfuric acid remains unhydrated whereas 37−58% forms a monohydrate, 2−12% a dihydrate, 1−29% a trihydrate, 0−3% a tetrahydrate, with negligible amounts of the larger hydrates. Figure 12 shows the predicted hydrate distributions and Table 7 contains the number concentrations. We find that the predicted extent of hydration is significantly smaller than experimental observations[60] as well as predictions of the CLD model[62] and other works.[72,74]

4. DISCUSSION

4.1. Basis Set Extrapolation Schemes. By using DF-MP2-F12/VQZ-F12 binding energies as a benchmark, we have evaluated the ability of Halkier's conventional scheme (eq 1)

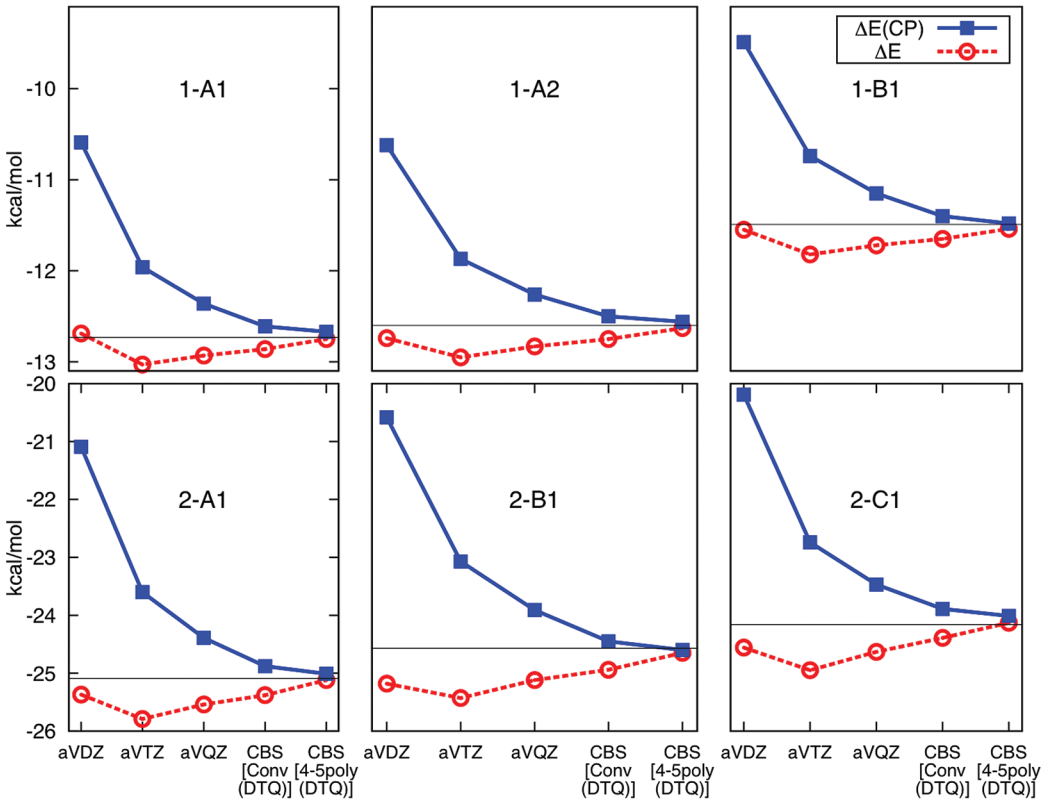

Figure 2. Convergence of the counterpoise (CP) corrected and uncorrected binding energies for six isomers of $H_2SO_4(H_2O)_{n=1,2}$ as a function of basis set and extrapolation scheme. The horizontal line corresponds to the benchmark DF-MP2-F12/VQZ-F12 binding energy.

Table 1. Effect of Anharmonic Corrections (kcal mol^{-1}) on the RI-MP2/CBS Binding Energies of Three Isomers of $H_2SO_4(H_2O)$ and $H_2SO_4(H_2O)_2$ in the Reaction $H_2SO_4 + n(H_2O) \rightarrow H_2SO_4(H_2O)_n$[a]

		$\Delta E(0)$			$\Delta H(298.15\ K)$			$\Delta G(298.15\ K)$			
n	isomer	harm	anharm	sc harm	harm	anharm	sc harm	harm	anharm	sc harm	expt
1	A1	−10.47	−10.62	−10.68	−11.11	−11.13	−11.17	−2.40	−2.80	−2.87	−3.6 ± 1[b]
1	A2	−10.32	−10.49	−10.52	−10.96	−11.00	−11.02	−2.27	−2.66	−2.73	
1	B1	−9.34	−9.48	−9.54	−9.92	−9.91	−9.97	−1.63	−2.04	−2.13	
2	A1(C_2)	−20.36	−20.63	−20.66	−21.71	−21.68	−21.74	−3.31	−4.16	−4.11	−5.9 ± 1.3[b]
2	B1	−19.47	−19.82	−19.77	−21.09	−21.18	−21.14	−1.95	−2.73	−2.67	
2	C1	−19.57	−19.97	−19.87	−20.94	−21.06	−20.96	−2.94	−3.79	−3.73	

[a]Harm = using harmonic frequencies; anharm = using VPT2 fundamental frequencies; sc harm = using scaling factors of 0.979, 1.077, and 1.102 for the ZPVE, $\Delta H_{vib}(T)$ and $S_{vib}(T)$. Enthalpies and free energies are for a standard state of 1 atm. [b]Reference 63.

and the 4-5 inverse polynomial extrapolation scheme (eq 2) to lead to the CBS limit. Figure 1 illustrates that the convergence of the binding energy to the CBS is not monotonic because of the incompleteness of the aVDZ basis set. The binding energy is not sufficiently converged even when the larger aVTZ, aVQZ, and aV5Z basis sets are used. Halkier's extrapolation scheme, designated as CBS[Conv(DTQ)] actually performs worse than the aV5Z basis set. In addition, using large basis sets in the extrapolation did not necessarily lead to better binding energies, as shown in Table S3, Supporting Information. The 4-5 inverse polynomial extrapolation, CBS[4-5poly(DTQ)], however, reproduces the DF-MP2-F12/VQZ-F12 binding energies almost exactly. We have observed similar results for water clusters,[93,94] where the 4-5 inverse polynomial scheme agreed with benchmark binding energies[93,95,115−118] much more closely than the conventional scheme. Furthermore, Figure 2 shows how the counterpoise corrected and uncorrected RI-MP2 binding energies converge to the same limit when extrapolated using the 4-5 inverse polynomial scheme. The CP corrected and uncorrected binding energies should theoretically converge to the same limit and the better extrapolation scheme is the one that leads to the fastest convergence to this limit.[115−118] The mean absolute difference between the ΔE[RI-MP2/CBS] and ΔE^{CP}[RI-MP2/CBS] is 0.08 kcal mol^{-1} for the 4-5 inverse polynomial extrapolation and 0.38 kcal mol^{-1} for the Halkier scheme based on the six isomers of $H_2SO_4(H_2O)_{n=1,2}$. In addition, the agreement between the ΔE[DF-MP2-F12/VQZ-F12] and the ΔE[RI-MP2/CBS] and ΔE^{CP}[RI-MP2/CBS] binding energies is remarkable for the 4-5 inverse polunomial extrapolation. Thus, we used the 4-5 inverse polynomial scheme with the aVDZ, aVTZ and aVQZ basis sets to extrapolate to the CBS limit in this work and all further reference to the CBS implies CBS[4-5poly(DTQ)].

The results presented in this paper demonstrate the importance of choosing a good basis set extrapolation scheme. The difference between the two schemes amounts to a kcal

dx.doi.org/10.1021/jp2119026 | J. Phys. Chem. A 2012, 116, 2209−2224

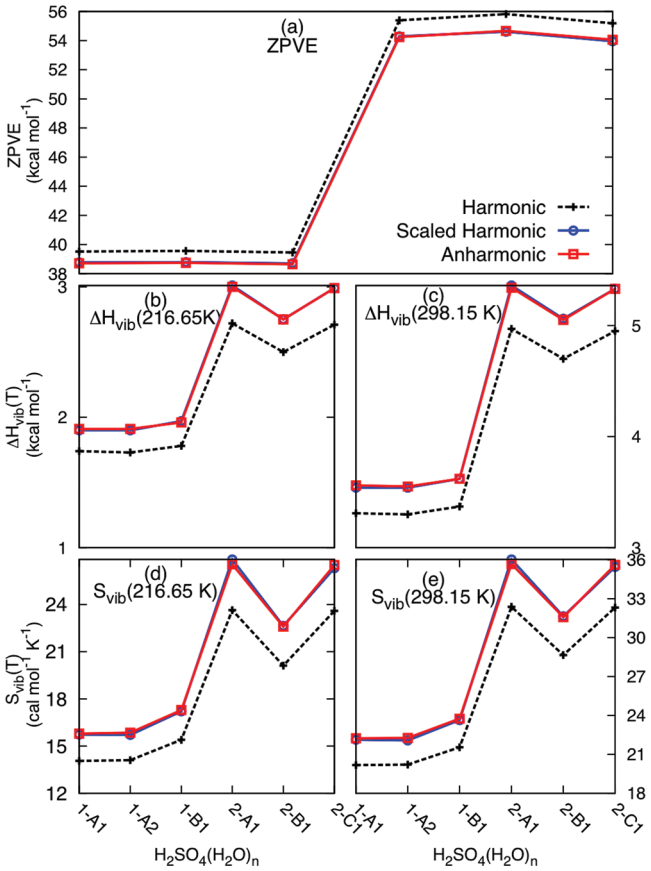

Figure 3. Comparison of the RI-MP2/aVDZ harmonic, scaled harmonic and anharmonic (a) ZPVE, (b) ΔH_{vib}(216.65 K), (c) ΔH_{vib}(298.15 K), (d) S_{vib}(216.65 K), and (e) S_{vib}(298.65 K) for six isomers of $H_2SO_4(H_2O)_{n=1,2}$.

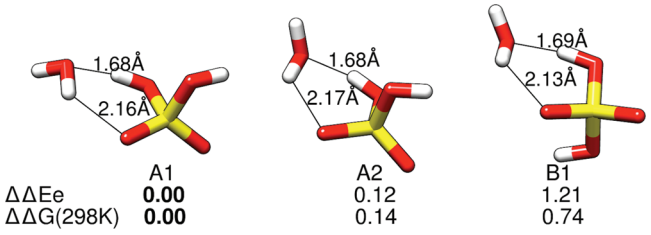

Figure 4. RI-MP2/CBS low energy isomers of $H_2SO_4(H_2O)$ sorted in order of increasing electronic energy (E_e) in kcal mol^{-1}.

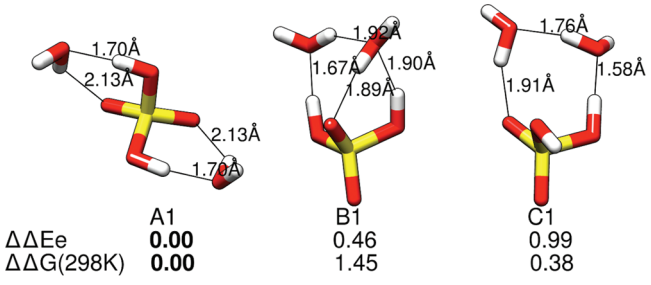

Figure 5. RI-MP2/CBS low energy isomers of $H_2SO_4(H_2O)_2$ sorted in order of increasing electronic energy (E_e) in kcal mol^{-1}.

mol^{-1} or more for the larger hydrates, which translates to enormous differences in cluster abundances and nucleation rates. Extrapolation schemes that rely heavily on the aVDZ basis sets will overestimate the binding energy because of the

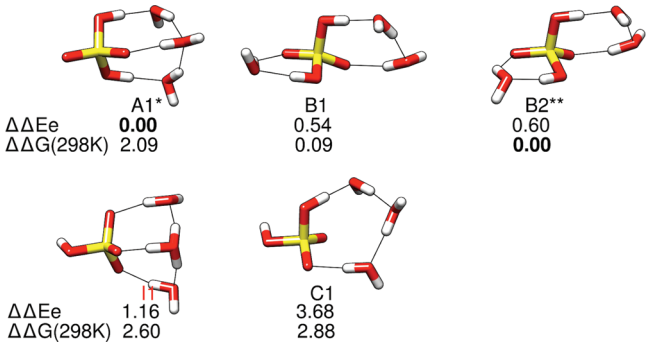

Figure 6. RI-MP2/CBS low energy isomers of $H_2SO_4(H_2O)_3$ sorted in order of increasing electronic energy (E_e) in kcal mol^{-1}. The * and ** indicate the E_e and G(298K) global minima.

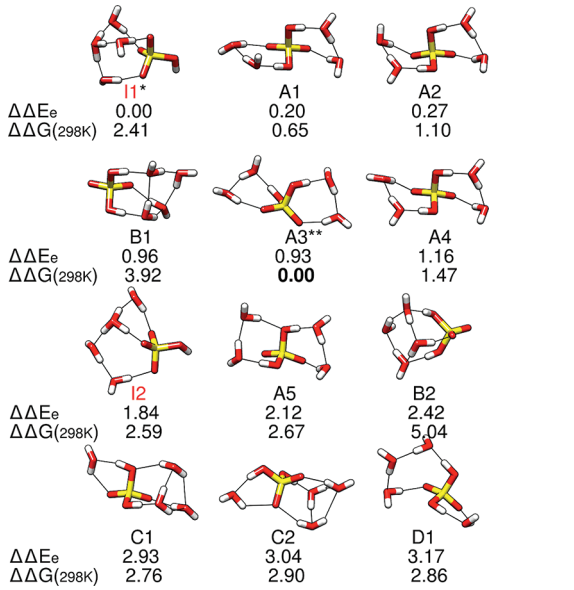

Figure 7. RI-MP2/CBS low energy isomers of $H_2SO_4(H_2O)_4$ sorted in order of increasing electronic energy (E_e) in kcal mol^{-1}. The * and ** indicate the E_e and G(298K) global minima.

nonmonotonic convergence of the binding energy. The aVDZ basis itself might yield binding energies that are close to the CBS because of a fortuitous cancellation of errors resulting from BSSE and BSIE. Kurtén recently highlighted the problem when including the aVDZ basis set in extrapolation schemes and suggested the use of explicitly correlated methods to overcome basis set incompleteness and superposition errors.[131]

4.2. Anharmonicity Corrections. VPT2 anharmonic frequencies serve as reliable proxies for experimental frequencies of hydrogen-bonded systems when experimental values are not available, as demonstrated for water clusters in our recent paper.[95] Comparing VPT2 fundamental frequencies with experimental ones for the water dimer (the only water cluster system whose vibrational spectrum is fully resolved), the VPT2 frequencies were found to be much closer to the experimental frequencies than the harmonic ones. Also, thermodynamic corrections calculated using the VPT2 frequencies were in better agreement with experimental[132] and benchmark theoretical[133] dimerization energies of water. Having validated the use of VPT2 fundamental frequencies for the water dimer, we used them to develop scaling factors for the ZPVE, $\Delta H_{vib}(T)$, and $\Delta S_{vib}(T)$ values for larger water clusters.

dx.doi.org/10.1021/jp2119026 | J. Phys. Chem. A 2012, 116, 2209–2224

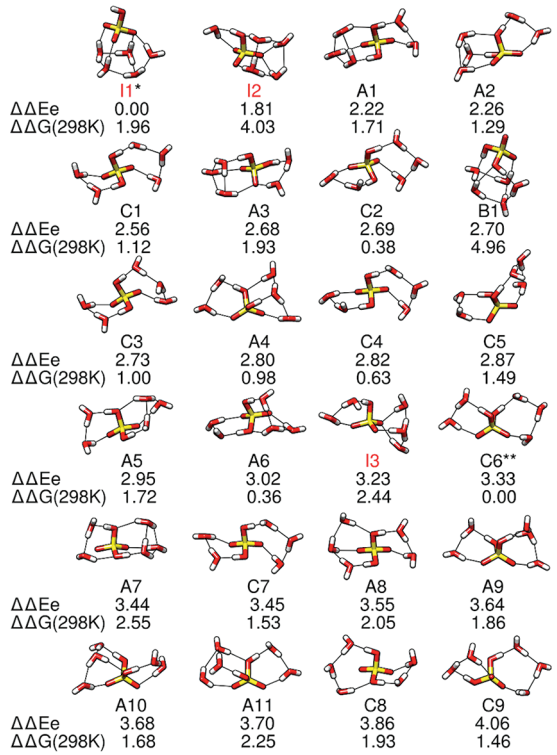

Figure 8. RI-MP2/CBS low energy isomers of $H_2SO_4(H_2O)_5$ sorted in order of increasing electronic energy (E_e) in kcal mol^{-1}. The * and ** indicate the E_e and G(298K) global minima.

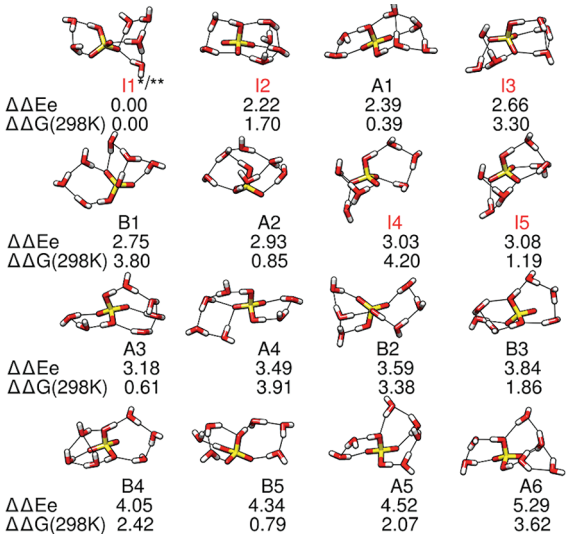

Figure 9. RI-MP2/CBS low energy isomers of $H_2SO_4(H_2O)_6$ sorted in order of increasing electronic energy (E_e) in kcal mol^{-1}. The * and ** indicate the E_e and G(298K) global minima.

For the case of sulfuric acid and its hydrates, the available experimental vibrational frequencies are incomplete and ambiguous in their assignments. Currently, only some of the experimental vibrational frequencies of the acid[134,135] and its monohydrate[136] are available. In the absence of extensive experimental vibrational spectra, calculated VPT2[74,128] and VSCF[137,138] anharmonic frequencies provide viable alternatives to correct for vibrational anharmonicity. Kurtén et al. have successfully used a similar approach to get anharmonic thermodynamic quantities for $H_2SO_4(H_2O)_{n=1-4}$ and $HSO_4^-(H_2O)_{n=1-4}$.[74] They calculated the anharmonic vibrational enthalpy and entropy using simple perturbation theory (SPT)[139] as well as a more rigorous treatment that includes the anharmonicity constants.[74] We chose to use SPT anharmonic vibrational enthalpies and entropies because the other approach has not been tested on any other system to date. By comparing the harmonic and SPT anharmonic thermodynamic corrections for six isomers of the monohydrate and dihydrate, we determined scaling factors for the ZPVE, $\Delta H_{vib}(T)$, and $S_{vib}(T)$, which we applied to all the clusters universally. The effect of these anharmonic corrections on the ZPVE, $\Delta H_{vib}(T)$, and $S_{vib}(T)$ of each cluster is sizable, as shown in Figure 3. They also lower the total $[H_2SO_4 + n(H_2O) \rightarrow H_2SO_4(H_2O)_n]$ and stepwise $[H_2SO_4(H_2O)_{n-1} + H_2O \rightarrow H_2SO_4(H_2O)_n]$ binding enthalpies and free energies noticeably. The Boltzmann averaged stepwise $\Delta G(T)$ changed from −0.47 to +0.15 kcal mol^{-1} whereas the total $\Delta G(T)$ decreased by 0.34−2.04 at T = 216.65−298.15 K. (See Table S4, Supporting Information, for harmonic thermodynamic values and Tables S5−S8, Supporting Information, for harmonic and VPT2 fundamental frequencies.)

4.3. Structures. In general, isomers with a *trans*-H_2SO_4 structure are more energetically favorable than those with a *cis*-H_2SO_4. This is reasonable as the *trans*-H_2SO_4 structure is 1.24 kcal mol^{-1} lower in electronic energy than *cis*-H_2SO_4 at the RI-MP2/CBS level of theory. The *cis*-H_2SO_4 isomer becomes increasingly favorable at higher temperatures because of its higher entropy. This is because the C_2 spatial symmetry of the *trans*-H_2SO_4 isomer lowers its rotational entropy by a factor of 2. At 298.15 K, the *cis*-H_2SO_4 isomer's free energy is only 0.26 kcal mol^{-1} higher than that of *trans*-H_2SO_4. The isomers with a *cis*-H_2SO_4 entity are also more likely to form three-dimensional hydrogen-bonding networks because both acidic hydrogens of the sulfuric acid are oriented on the same side. Those with a *trans*-H_2SO_4 moiety form quasi-planar networks composed largely of single donor-single acceptor (DA) water monomers. There are a variety of hydrogen bonds featured in these clusters. Each water monomer either forms a DA, DDA (double donor-single acceptor), or DAA (single donor-double acceptor) hydrogen bond with the sulfuric acid, other waters, or both. For the smaller and quasi-planar clusters, DA waters are common, but DAA and DDA waters become more ubiquitous as the clusters grow. The presence of a *cis*-H_2SO_4 or deprotonated H_2SO_4 favors the formation of more cage-like 3-D hydrogen bond networks, hence more DAA and DDA motifs.

The primary hydrogen bonds between an acidic proton of sulfuric acid and an acceptor water are typically strong, as they are characterized by short hydrogen bond lengths and angles approaching linearity.[140] The secondary hydrogen bonds where the sulfuric acid oxygen is the acceptor are typically longer, weaker, and highly bent. For the case of the A1 and A2 isomers of the monohydrate, the strength of the primary and secondary hydrogen bonds was estimated by Rozenberg and Loewenschuss to be 8−9 and 3−4 kcal mol^{-1}, respectively.[141] The hydrogen bond distances shown for $H_2SO_4(H_2O)_{n=1,2}$ in Figures 4 and 5 clearly show the difference in these two types of hydrogen bonds. Because of the varying nature and strength of the hydrogen bonds that can form, the correlation between number of hydrogen bonds and enthalpic stability is not always exact. However, the notion that isomers with fewer hydrogen bonds are more entropically favorable holds true on a consistent basis.

dx.doi.org/10.1021/jp2119026 | J. Phys. Chem. A 2012, 116, 2209−2224

Table 2. RI-MP2/CBS[a] Scaled Harmonic[b] Binding Energies for $H_2SO_4(H_2O)_{n=1-3}$[c]

				216.65 K		273.15 K		298.15 K	
n	isomer	CBS ΔE_e[RI-MP2]	0 K ΔE	ΔH	ΔG	ΔH	ΔG	ΔH	ΔG
1	A1	**−12.75**	**−10.68**	**−11.26**	**-5.15**	**−11.20**	**−3.56**	**−11.17**	**−2.87**
1	A2	−12.63	−10.52	−11.11	−5.01	−11.06	−3.43	−11.02	−2.73
1	B1	−11.54	−9.54	−10.07	−4.29	−10.01	−2.79	−9.97	−2.13
2	A1(C_2)	**−25.12**	**−20.66**	**−21.88**	**−8.96**	**−21.80**	**−5.59**	**−21.74**	**−4.11**
2	B1	−24.66	−19.77	−21.24	−7.73	−20.92	−5.09	−21.14	−2.67
2	C1	−24.13	−19.87	−21.09	−8.47	−21.28	−4.31	−20.96	−3.73
3	A1	**−37.67**	−30.28	**−32.46**	−12.23	**−32.41**	−6.95	**−32.35**	−4.63
3	B1	−37.13	−30.44	−32.30	−13.65	−32.21	−8.77	−32.13	−6.62
3	B2	−37.07	**−30.45**	−32.29	**−13.72**	−32.20	**−8.85**	−32.11	**−6.71**
3	I1	−36.50	−29.70	−32.02	−11.77	−32.11	−6.46	−32.11	−4.11
3	C1	−33.99	−27.70	−29.48	−10.86	−29.40	−5.98	−29.32	−3.84

[a]RI-MP2/aVDZ, RI-MP2/aVTZ, and RI-MP2/aVQZ binding energies extrapolated using eq 2. [b]ZPVE, ΔH_{vib}(216.65 K), ΔH_{vib}(273.15 K), ΔH_{vib}(298.15 K), S_{vib}(216.65 K), S_{vib}(273.15 K), and S_{vib}(298.15 K) scaled by 0.979, 1.101, 1.083, 1.077, 1.123, 1.108, and 1.102, respectively. [c]All energies are in kcal mol^{-1}. Global minima shown in bold. Enthalpies and free energies are for a standard state of 1 atm.

Table 3. RI-MP2/CBS[a] Scaled Harmonic[b] Binding Energies for $H_2SO_4(H_2O)_4$[c]

				216.65 K		273.15 K		298.15 K	
n	isomer	CBS ΔE[RI-MP2]	0 K ΔE	ΔH	ΔG	ΔH	ΔG	ΔH	ΔG
4	I1	**−49.54**	−40.17	−42.78	**−16.84**	**−43.39**	−8.62	**−43.38**	−5.43
4	A1	−49.34	**−40.29**	−42.93	−16.71	−42.81	−10.18	−42.72	−7.19
4	A2	−49.27	−40.21	**−43.14**	−15.78	−42.75	−9.77	−42.66	−6.75
4	B1	−48.58	−38.66	−41.12	−16.16	−41.55	−7.08	−41.48	−3.93
4	A3	−48.61	−39.75	−42.30	−16.41	−42.11	**−10.73**	−42.01	**−7.84**
4	A4	−48.37	−39.47	−42.58	−15.10	−41.91	−9.35	−41.81	−6.37
4	I2	−47.70	−38.73	−41.28	−15.23	−41.61	−8.31	−41.58	−5.25
4	A5	−47.42	−38.47	−41.40	−14.38	−40.92	−8.17	−40.82	−5.17
4	B2	−47.11	−37.07	−39.59	−13.92	−39.97	−5.92	−39.90	−2.80
4	C1	−46.61	−37.86	−40.35	−14.73	−40.22	−8.04	−40.11	−5.09
4	C2	−46.50	−37.76	−40.61	−14.25	−40.16	−7.91	−40.06	−4.95
4	D1	−46.37	−37.49	−39.92	−14.54	−39.80	−7.91	−39.69	−4.98

[a]RI-MP2/aVDZ, RI-MP2/aVTZ, and RI-MP2/aVQZ binding energies extrapolated using eq 2. [b]ZPVE, ΔH_{vib}(216.65 K), ΔH_{vib}(273.15 K), ΔH_{vib}(298.15 K), S_{vib}(216.65 K), S_{vib}(273.15 K), and S_{vib}(298.15 K) scaled by 0.979, 1.101, 1.083, 1.077, 1.123, 1.108, and 1.102, respectively. [c]All energies are in kcal mol^{-1}. Global minima shown in bold. Enthalpies and free energies are for a standard state of 1 atm.

The dissociation of a hydrated H_2SO_4−H_2O moiety into hydrated HSO_4^-−H_3O^+ ion pairs is one of the many interesting features of sulfuric acid hydrates. Considering that sulfuric acid is a strong acid, it is expected to completely dissociate in aqueous solutions, and the first $[H_2SO_4(H_2O)_n \rightarrow HSO_4^-H_3O^+(H_2O)_{n-1}]$ deprotonation happens even in the gas phase in the presence of a few waters. This dissociation is hard to capture using classical force fields that are not properly parametrized[68,142] and none of the structures we sampled from our MD simulation contained ion pairs. Classical Monte Carlo simulations by Kusaka et al.[42] found no ion pair formation for small sulfuric acid hydrates. However, numerous DFT and ab initio methods have predicted this ion pair formation, or deprotonation of H_2SO_4, to occur at different cluster sizes depending on the temperature. Arstila et al.[65] used DFT to predict that ion pair formation starts with n = 3. Bandy and Ianni[66] also used DFT to predict that $H_2SO_4(H_2O)_{n=3-7}$ form ion pair clusters, and are the global minima in terms of E_e and G(298.15 K) when $n \geq 4$ and $n \geq 8$, respectively. Re et al.[67] suggested that ionic pair clusters are more stable than neutral clusters when $n \geq 3$ and $n \geq 5$; Ding et al.[68,69] similarly predicted the coexistence of neutral and ionic pair clusters for $n \geq 3$ using their model potentials. Sugawara et al.[143] used path integral molecular dynamics (PIMD) with a semiempirical potential and concluded that the first and second deprotonation of sulfuric acid starts at n = 4 and n = 10−12, respectively, at 300 K.[143] Our calculations show that the ionic pair clusters become the E_e and G(298.15 K) global minima when $n \geq 4$ and n = 6. The overall energetic stabilization brought upon by the formation of ion pairs is not significant. As a result, the upward trend of the stepwise binding free energy with increasing number of waters proceeds unabated for $n \geq 4$. For clusters with more than one sulfuric acid, the ion pair formation involving least one sulfuric acid occurs even in the presence of just two waters.[144]

4.4. Thermodynamics of Forming $H_2SO_4(H_2O)_n$. Different density functionals (LDA,[65] B3LYP,[66,67,73] and PW91[70]) have been used to study the thermodynamics of sulfuric acid hydrate formation with varying degrees of success. Despite their attractive computational cost and reasonably good performance for hydrogen-bonded systems, there are many downsides to using DFT methods. First, there is no systematic way of improving their performance by employing either a better description of the one-particle basis sets or the n-particle electron correlation. Second, they do not capture important dispersion interactions well without explicit corrections or

dx.doi.org/10.1021/jp2119026 | J. Phys. Chem. A 2012, 116, 2209−2224

Table 4. RI-MP2/CBS[a] Scaled Harmonic[b] Binding Energies for $H_2SO_4(H_2O)_5$[c]

				216.65 K		273.15 K		298.15 K	
n	isomer	CBS ΔE[RI-MP2]	0 K ΔE	ΔH	ΔG	ΔH	ΔG	ΔH	ΔG
5	I1	**−61.41**	**−49.20**	**−53.05**	−18.35	**−53.13**	−9.28	**−53.10**	−5.26
5	I2	−59.60	−47.24	−50.56	−17.48	−51.19	−7.21	−51.15	−3.19
5	A1	−59.18	−47.89	−51.16	−18.46	−51.10	−9.48	−50.99	−5.67
5	A2	−59.14	−47.89	−51.21	−18.27	−51.04	−9.91	−50.92	−6.14
5	C1	−58.84	−47.66	−51.55	−16.73	−50.69	−10.06	−50.57	−6.33
5	A3	−58.73	−47.50	−51.30	−16.73	−50.73	−9.27	−50.62	−5.47
5	C2	−58.72	−47.73	−50.88	−18.58	−50.62	−10.80	−50.50	−7.14
5	B1	−58.70	−46.09	−49.12	−17.44	−49.89	−6.28	−49.81	−2.29
5	C3	−58.67	−47.64	−50.73	−18.59	−50.59	−10.18	−50.47	−6.47
5	A4	−58.61	−47.90	−50.97	−19.24	−50.85	−10.19	−50.72	−6.47
5	C4	−58.59	−47.52	−50.68	−18.31	−50.45	−10.55	−50.33	−6.89
5	C5	−58.54	−47.37	−50.46	−18.11	−50.40	−9.69	−50.28	−5.96
5	A5	−58.45	−47.33	−50.52	−17.97	−50.39	−9.46	−50.27	−5.71
5	A6	−58.38	−47.56	−50.55	−19.06	−50.40	−10.82	−50.27	−7.19
5	I3	−58.18	−47.34	−50.54	−17.75	−50.87	−8.76	−50.80	−4.90
5	C6	−58.08	−47.14	−50.11	**−19.27**	−49.97	**−11.18**	−49.84	**−7.62**
5	A7	−57.97	−46.80	−49.85	−17.85	−49.88	−8.64	−49.76	−4.86
5	C7	−57.96	−46.96	−50.10	−17.75	−49.86	−9.64	−49.73	−5.95
5	A8	−57.85	−46.84	−49.98	−17.59	−49.84	−9.12	−49.72	−5.39
5	A9	−57.77	−46.75	−49.86	−17.72	−49.70	−9.32	−49.57	−5.62
5	A10	−57.73	−46.89	−49.92	−17.87	−49.76	−9.49	−49.63	−5.80
5	A11	−57.71	−46.60	−50.13	−16.76	−49.61	−8.93	−49.48	−5.20
5	C8	−57.54	−46.55	−49.58	−17.61	−49.43	−9.24	−49.30	−5.56
5	C9	−57.35	−46.38	−49.45	−17.97	−49.32	−9.72	−49.20	−6.09

[a]RI-MP2/aVDZ, RI-MP2/aVTZ, and RI-MP2/aVQZ binding energies extrapolated using eq 2. [b]ZPVE, ΔH_{vib}(216.65 K), ΔH_{vib}(273.15 K), ΔH_{vib}(298.15 K), S_{vib}(216.65 K), S_{vib}(273.15 K), and S_{vib}(298.15 K) scaled by 0.979, 1.101, 1.083, 1.077, 1.123, 1.108, and 1.102, respectively. [c]All energies are in kcal mol^{-1}. Global minima shown in bold. Enthalpies and free energies are for a standard state of 1 atm

Table 5. RI-MP2/CBS[a] Scaled Harmonic[b] Binding Energies for $H_2SO_4(H_2O)_6$[c]

				216.65 K		273.15 K		298.15 K	
n	isomer	CBS ΔE[RI-MP2]	0 K ΔE	ΔH	ΔG	ΔH	ΔG	ΔH	ΔG
6	I1	**−71.35**	**−57.47**	**−61.78**	**−21.81**	**−61.81**	**−11.33**	**−61.73**	**−6.70**
6	I2	−69.13	−55.21	−59.12	−19.59	−59.72	−8.07	−59.65	−3.34
6	A1	−68.96	−55.37	−59.12	−20.49	−59.14	−9.41	−59.00	−4.86
6	I3	−68.69	−54.90	−58.90	−18.63	−59.29	−7.49	−59.21	−2.74
6	B1	−68.60	−55.52	−59.98	−19.09	−59.11	−10.53	−58.96	−6.08
6	A2	−68.42	−54.52	−58.21	−19.75	−58.40	−7.73	−58.26	−3.09
6	I4	−68.33	−54.93	−59.32	−18.25	−59.13	−8.49	−59.04	−3.85
6	I5	−68.28	−54.70	−58.43	−19.86	−58.97	−7.82	−58.88	−3.13
6	A3	−68.17	−55.01	−58.65	−20.60	−58.52	−10.18	−58.36	−5.74
6	A4	−67.86	−54.61	−58.89	−18.34	−58.17	−9.67	−58.02	−5.22
6	B2	−67.76	−54.63	−58.85	−18.71	−58.11	−10.26	−57.95	−5.87
6	B3	−67.51	−54.44	−58.07	−19.50	−57.89	−9.41	−57.73	−4.97
6	B4	−67.30	−54.17	−57.86	−19.01	−57.68	−8.85	−57.53	−4.37
6	B5	−67.01	−54.11	−57.61	−20.27	−57.42	−10.48	−57.26	−6.17
6	A5	−66.83	−53.77	−57.36	−19.20	−57.18	−9.21	−57.03	−4.80
6	A6	−66.06	−52.89	−56.52	−17.77	−56.32	−7.64	−56.15	−3.18

[a]RI-MP2/aVDZ, RI-MP2/aVTZ, and RI-MP2/aVQZ binding energies extrapolated using eq 2. [b]ZPVE, ΔH_{vib}(216.65 K), ΔH_{vib}(273.15 K), ΔH_{vib}(298.15 K), S_{vib}(216.65 K), S_{vib}(273.15 K), and S_{vib}(298.15 K) scaled by 0.979, 1.101, 1.083, 1.077, 1.123, 1.108, and 1.102, respectively. [c]All energies are in kcal mol^{-1}. Global minima shown in bold. Enthalpies and free energies are for a standard state of 1 atm.

heavy parametrization.[91,145,146] We opted to use MP2 theory because it describes hydrogen bonded systems well and can be extrapolated systematically to its complete basis set limit when used with correlation consistent basis sets.[74,92−94]

Because these clusters are held together by flexible and highly dynamic hydrogen bonds, the barrier to the transformation of one isomer to another should be very low. At ambient temperatures, it is expected that an ensemble of isomers would be present for each hydrate size. To account for the contribution of different isomers, we have Boltzmann averaged the $\Delta H(T)$ and $\Delta G(T)$ for each hydrate size over the low energy isomers described in this study. Naturally, including the

dx.doi.org/10.1021/jp2119026 | J. Phys. Chem. A 2012, 116, 2209−2224

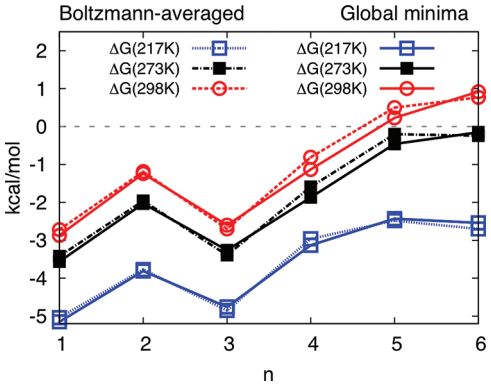

Figure 10. Comparison of the Boltzmann averaged (dotted lines) and global minimum (solid lines) RI-MP2/CBS scaled harmonic thermodynamics of stepwise $[H_2SO_4(H_2O)_{n-1} + H_2O \rightarrow H_2SO_4(H_2O)_n]$ sulfuric acid hydrate growth. Boltzmann averaging over an ensemble of low energy isomers has a minimal effect on the $\Delta G(T)$ of hydration.

contributions of the higher energy isomers would raise the $\Delta H(T)$ and $\Delta G(T)$ slightly compared to only looking at the global minimum isomer. That is precisely what we see in Figure 10 where the $\Delta G(T)$ of stepwise hydration changes vary little whether we use the $\Delta G(T)$ of the global minima only or Boltzmann average over the ensemble of low energy isomers.

As shown at the top of Figure 11, the formation of sulfuric acid hydrates by the stepwise addition of water monomers is an exothermic reaction, and it is favorable over the temperature range spanned by the troposphere. Accounting for entropic effects changes that picture dramatically. The bottom of Figure 11 demonstrates that the free energy of association of water with sulfuric acid is favorable up to size $n = 6$ at $T = 216.65-273.15$ K, but not at higher temperatures; specifically at 298.15 K, only clusters of size $n = 1-4$ have favorable thermodynamics. This does not imply that clusters with five to six waters would never form, but rather one would find a much smaller number of these bigger hydrates compared to those with one to four

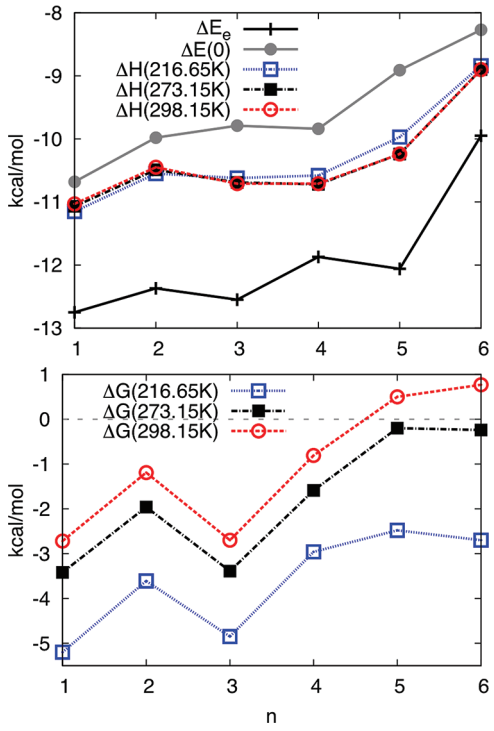

Figure 11. RI-MP2/CBS Boltzmann averaged scaled harmonic thermodynamics of stepwise $[H_2SO_4(H_2O)_{n-1} + H_2O \rightarrow H_2SO_4(H_2O)_n]$ sulfuric acid hydrate growth.

waters at equilibrium. The exact values depend on the initial concentrations of water and sulfuric acid as well as the temperature and pressure. At lower temperatures, the lesser entropic penalty for forming these hydrates keeps the $\Delta G(T)$ negative, even though it is clearly trending upward.

These results are in general agreement with Kurtén et al.'s[74] prior ab initio work on $H_2SO_4(H_2O)_{n=1-4}$, but quantitative differences do remain. Comparing the electronic binding energies (ΔE), they report values for their lowest energy

Table 6. RI-MP2/CBS[a] Boltzmann Averaged[b] Scaled Harmonic[c] Binding Energy of Sulfuric Acid Hydrates[d]

			216.65 K		273.15 K		298.15 K	
n	CBS ΔE[RI-MP2]	0 K ΔE	ΔH	ΔG	ΔH	ΔG	ΔH	ΔG
			$H_2SO_4 + n(H_2O) \rightarrow H_2SO_4(H_2O)_n$					
1	−12.75	−10.68	−11.16	−5.03	−11.07	−3.42	−11.02	−2.72
2	−25.12	−20.66	−21.68	−8.79	−21.56	−5.38	−21.48	−3.91
3	−37.67	−30.45	−32.32	−13.65	−32.25	−8.77	−32.19	−6.61
4	−49.34	−40.29	−42.88	−16.60	−42.97	−10.36	−42.89	−7.42
5	−61.41	−49.20	−52.84	−18.89	−52.75	−10.58	−52.61	−6.94
6	−71.35	−57.47	−61.72	−21.59	−61.64	−10.82	−61.50	−6.17
			$H_2SO_4(H_2O)_{n-1} + H_2O \rightarrow H_2SO_4(H_2O)_n$					
1	−12.75	−10.68	−11.16	−5.03	−11.07	−3.42	−11.02	−2.72
2	−12.37	−9.98	−10.53	−3.76	−10.49	−1.96	−10.45	−1.19
3	−12.55	−9.79	−10.64	−4.86	−10.69	−3.39	−10.71	−2.70
4	−11.68	−9.84	−10.57	−2.95	−10.72	−1.59	−10.71	−0.81
5	−12.06	−8.91	−9.95	−2.29	−9.78	−0.22	−9.71	0.48
6	−9.95	−8.27	−8.89	−2.69	−8.90	−0.24	−8.90	0.77

[a]RI-MP2/aVDZ, RI-MP2/aVTZ, and RI-MP2/aVQZ binding energies extrapolated using eq 2. [b]ΔH(216.65 K), ΔH(273.15 K), ΔH(298.15 K), ΔG(216.65 K), ΔG(273.15 K), and ΔG(298.15 K) Boltzmann averaged over low energy isomers. [c]ZPVE, ΔH_{vib}(216.65 K), ΔH_{vib}(273.15 K), ΔH_{vib}(298.15 K), S_{vib}(216.65 K), S_{vib}(273.15 K), and S_{vib}(298.15 K) scaled by 0.979, 1.101, 1.083, 1.077, 1.123, 1.108, and 1.102, respectively. [d]All energies are in kcal mol^{-1}. Enthalpies and free energies are for a standard state of 1 atm

dx.doi.org/10.1021/jp2119026 | J. Phys. Chem. A 2012, 116, 2209−2224

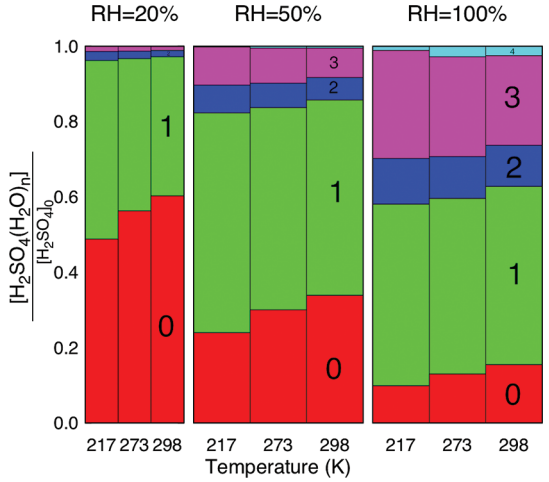

Figure 12. Equilibrium sulfuric acid hydrate distribution assuming a saturation (100% RH) vapor pressure of $[H_2O] = 9.9 \times 10^{14}$, 1.6×10^{17}, and 7.7×10^{17} cm^{-3} at T = 216.65, 273.15, and 298.15 K, respectively, and $[H_2SO_4]_0 = 5 \times 10^7$ cm^{-3}. $H_2SO_4(H_2O)_{n=5,6}$ do not form in large enough numbers to be seen on this plot.

isomer that are typically about 0.4−0.6 kcal mol^{-1} lower than ours for $H_2SO_4(H_2O)_{n=1-4}$. One reason for the difference is their inclusion of an MP4 additive correction to the MP2 binding energy whereas we opted not to incorporate any post-MP2 electron correlation correction because it is not rigorously additive for hydrogen-bonded systems. Most of the remaining difference can be attributed primarily to their use of an inverse cubic extrapolation, whereas we employed the 4-5 inverse polynomial (eq 2); the extra d-function on the aV(N+d)Z basis set of sulfur has virtually no effect on the binding energies compared to aVNZ, as demonstrated in Table S2, Supporting Information. In section 4.1 we explained why including the aVQZ basis set and using the 4-5 inverse polynominal extrapolation scheme should yield more accurate electronic binding energies. The differences in the harmonic ΔH(298.15 K) and ΔG(298.15 K) values (see Table S3, Supporting Information) are a combination of the above-mentioned basis set and correlation effects on the electronic energies, and proper accounting of the spatial symmetry of the clusters in calculating their rotational entropy. In particular, the *trans*-H_2SO_4 isomer has a C_2 spatial symmetry and a corresponding rotational symmetry number (σ) of 2. Its rotational entropy is thus half what it would be if its spatial symmetry is not taken into account (σ = 1). Factoring in the spatial symmetry of the *trans*-H_2SO_4 isomer effectively increases its G(298.15 K) and the ΔG(298.15 K) of all the clusters by 0.4 kcal mol^{-1}. The only hydrate that has high spatial symmetry is the A1 isomer of the dihydrate, which has C_2 symmetry. Once again, accounting for this symmetry increases the ΔG(298.15 K) of the A1 dihydrate by about 0.4 kcal mol^{-1}. Further differences for $H_2SO_4(H_2O)_{n=3,4}$ result from different global minima. Differences between their SPT anharmonic ΔH(298.15 K) and ΔG(298.15 K) and our scaled harmonic analogs are essentially due to the above-mentioned effects. Kurtén et al. report SPT anharmonic ΔH(298.15 K) values for their lowest energy isomers to be −11.50, −11.10, −11.07, and −11.18 kcal mol^{-1} for $H_2SO_4(H_2O)_{n=1-4}$ compared to −11.17, −10.57, −10.61, and −11.02 kcal mol^{-1} in our case. Similarly, the SPT anharmonic ΔG(298.15 K) for their lowest energy isomers are −3.30, −2.35, −2.69, and −1.21 kcal mol^{-1} compared to −2.87, −1.24, −2.60, and −1.13 kcal mol^{-1} in our case for $H_2SO_4(H_2O)_{n=1-4}$. Thus, our calculated thermodynamic values exhibit a similar trend to those of Kurtén et al.,[74] but differ quantitatively.

Getting reliable experimental thermodynamic quantities for the formation of small hydrogen bonded gas-phase clusters is very challenging. Currently, the only experimental estimate for ΔG(298.15 K) of successive hydration of H_2SO_4 comes from work by Hanson and Eisele[63] who indirectly determined the equilibrium constants of forming $H_2SO_4(H_2O)$ and $H_2SO_4(H_2O)_2$ from the first-order wall loss of H_2SO_4 passing through a cylindrical flow tube in an N_2 carrier gas at varying RH values. They attribute the decrease in the diffusion coefficient of H_2SO_4 with increasing RH to the formation of $H_2SO_4(H_2O)$ and $H_2SO_4(H_2O)_2$ even though they do not rule out the presence of bigger hydrates. The assumption that only $H_2SO_4(H_2O)$ and $H_2SO_4(H_2O)_2$ form predominantly at low RH (<40%) is not consistent with our calculated free energies, which suggests that $H_2SO_4(H_2O)_3$ should be more abundant than $H_2SO_4(H_2O)_2$ even at low RH (Figure 12), a consequence of its lower free energy (−2.70 kcal mol^{-1} for the trihydrate compared to −1.19 kcal mol^{-1} for the dihydrate). Some of these uncertainties notwithstanding, they report ΔG(298.15 K) values for the first and second hydration of H_2SO_4 to be −3.6 ± 1 and −2.3 ± 0.3 kcal mol^{-1}. Kurtén et al.[74] were successful in reproducing these results, but because their calculations lacked a rigorous basis set extrapolation and a proper account of spatial symmetry, one might have less confidence in the quality of their agreement with experiment. Our Gibbs free energies at

Table 7. Abundance of Sulfuric Acid Hydrates at 216.65, 273.15, and 298.15 K and Relative Humidity Values of 20%, 50%, and 100%[a]

	216.65 K			273.15 K			298.15 K		
n	RH = 20	RH = 50	RH = 100	RH = 20	RH = 50	RH = 100	RH = 20	RH = 50	RH = 100
0	2.4×10^7	1.2×10^7	5.0×10^6	2.8×10^7	1.5×10^7	6.5×10^6	3.0×10^7	1.7×10^7	7.7×10^6
1	2.4×10^7	2.9×10^7	2.4×10^7	2.0×10^7	2.7×10^7	2.3×10^7	1.9×10^7	2.6×10^7	2.4×10^7
2	1.2×10^6	3.7×10^6	6.1×10^6	9.8×10^5	3.2×10^6	5.6×10^6	8.6×10^5	3.0×10^6	5.5×10^6
3	7.3×10^5	5.0×10^6	1.4×10^7	6.4×10^5	4.6×10^6	1.3×10^7	5.1×10^5	3.9×10^6	1.2×10^7
4	5.5×10^3	9.0×10^4	5.0×10^5	1.5×10^4	2.5×10^5	1.4×10^6	1.2×10^4	2.2×10^5	1.3×10^6
5	8.5×10^0	3.2×10^2	3.4×10^3	2.7×10^1	1.0×10^3	1.1×10^4	3.0×10^1	1.2×10^3	1.4×10^4
6	2.6×10^{-2}	2.1×10^0	4.3×10^1	3.8×10^{-2}	3.2×10^0	6.5×10^1	3.6×10^{-2}	3.2×10^0	6.7×10^1

[a]Abundances given in molecules cm^{-3}. $[H_2SO_4]_0 = 5.0 \times 10^7$ cm^{-3} and $[H_2O] = 9.9 \times 10^{14}$, 1.6×10^{17}, and 7.7×10^{17} cm^{-3} at T = 216.65, 273.15, and 298.15 K, respectively, at saturation (100% RH). Using Boltzmann averaged RI-MP2/CBS ΔG(216.65 K), ΔG(273.15 K), and ΔG(298.15 K) shown at the bottom of Table 6.

dx.doi.org/10.1021/jp2119026 | J. Phys. Chem. A 2012, 116, 2209−2224

298.15 K for $n = 1$ are within the experimental error of Hanson and Eisele. Because our free energies were more positive than the experimental value for $n = 1, 2$, it is possible that Hanson and Eisele had a systematic error that lowered their value of the equilibrium constant used to calculate $\Delta G(298.15\ K)$.

The disagreement between the current and previous works highlights the difficulty of obtaining accurate thermodynamic quantities for hydrogen-bonded systems from theory or experiment. This work should be robust by virtue of its inclusion of large configurational sampling, more rigorous energy calculations, basis set extrapolations, and anharmonicity correction. The reliability of the RRHO framework for thermal corrections of hydrogen-bonded systems is a subject of some debate. Kathmann et al.[147] have argued that accounting for "(1) local anharmonicity of the vibrations for a given cluster configuration and (2) global anharmonicity resulting from sampling between the large number of configurations available within the relevant volume of configuration space" is necessary to get accurate cluster thermodynamics. In a computationally feasible way, we have addressed the question of local anharmonicity by introducing scaling factors and global anharmonicity by Boltzmann averaging over many low energy configurations.

4.5. Abundance of $H_2SO_4(H_2O)_n$ at Ambient Conditions. One systematic way to predict the atmospheric concentration of a given cluster using quantum chemistry[78] is through a stepwise building up of the cluster by adding a water molecule to each $H_2SO_4(H_2O)_{n-1}$ cluster to form $H_2SO_4(H_2O)_n$. The concentration of each hydrate will depend upon the concentration of the precursor $H_2SO_4(H_2O)_{n-1}$ hydrate, the concentration of water, and the thermodynamics of adding another water to the cluster. When adding another water molecule to the $H_2SO_4(H_2O)_{n-1}$ cluster is favored by free energy, the concentration of $H_2SO_4(H_2O)_n$ relative to $H_2SO_4(H_2O)_{n-1}$ hydrates increases, but once the addition of another water molecule is no longer favored, the equilibrium shifts toward the smaller cluster and the concentration of the larger cluster decreases.

Using the RI-MP2/CBS scaled harmonic free energies reported in Table 6, we calculated the concentration of $H_2SO_4(H_2O)_n$ with a standard state of 1 atm and $T = 216.65$, 273.15 and 298.15 K for $n = 1-6$ waters by solving the equilibrium equations for the system. The saturation vapor pressure of water vapor is given by Seinfeld and Pandis,[5] and it corresponds to a number concentration of 9.89×10^{14}, 1.62×10^{17}, and 7.70×10^{17} cm^{-3} at the three temperatures. The concentration of sulfuric acid in the atmospheric varies on the basis of time and geography. Berndt et al. have shown that the concentration of sulfuric acid made in a flow tube through a mechanism that is typical in the atmosphere needs to be above $\sim 10^7$ cm^{-3} for nucleation to take place.[23] We have thus used a sulfuric acid concentration of 5×10^7 cm^{-3}. Because the concentration of water vapor is much larger than that of sulfuric acid, it is assumed to remain unchanged by the hydration of the acid.

Table 7 lists the number concentration of the hydrates, and Figure 12 shows their composition as a fraction of the initial H_2SO_4, $[H_2SO_4]_0$, at three different temperature and RH values. Figure 12 reveals that 49–60% of the sulfuric acid is unhydrated at 20% RH, but that number decreases to 24–34% at 50% RH and 10–16% at 100% RH. The most common clusters are the monohydrates, and they make up 37–58% followed by the trihydrates (1–29%) and dihydrates (2–12%). Tetrahydrates are virtually nonexistent at 20% RH but form as much as 3% of the hydrates at 100% RH. The larger ($n > 5$) hydrates form in very low abundances. Even though the saturation vapor pressure of water decreases with temperature, the formation of hydrates is still most favorable at lower temperatures. As such, the highest number of hydrates are found at the tropopause ($T = 216.65$ K) at 100% RH, as shown in Figure 12.

The extent of hydration we report is much less than what has been predicted by CLD[31,48] and experimental reports.[60] Even at low relative humidities, sulfuric acid has been reported to form hydrates overwhelmingly,[60] whereas our results suggest that 50–60% of it remains unhydrated at 20% RH. Considering that hydration decreases nucleation rates by a factor of 10^3–10^8,[48] one of the reasons for the discrepancy between theoretical predictions and experimental new particle formation rates could be the overestimation of sulfuric acid hydration in CNT and other improved models.[48,49,54,61,64,148] Our ab initio calculations predict significantly different hydration of sulfuric acid than CLD,[31] DFT[65−72] methods as well as other theoretical works.[72,74] (See Figure S1, Supporting Information, for a comparison of CLD and RI-MP2/CBS hydration free energies)

4.6. Atmospheric Implications. It has been suggested that H_2SO_4–H_2O binary nucleation can explain observed new particle formation rates at ambient concentrations of H_2SO_4 ($\sim 10^5$–10^7 cm^{-3}) as long as the experimental techniques used can accurately measure the gaseous H_2SO_4 and efficiently detect small (<1.5 nm in diameter) particles.[21] By looking at the dependence of the nucleation rate on the concentration of the H_2SO_4 precursor, the authors concluded that the critical nuclei of this binary system must have one or two H_2SO_4 molecules. Recent studies have determined that some limitations of chemical ionization mass spectrometry (CIMS), and the presence of other species, like ammonia and amines, in trace amounts explains the low dependence of the nucleation rate on the concentration of H_2SO_4.[1,149] Thus, binary nucleation by itself is not sufficient to achieve observed new particle formation rates under ambient conditions.[59] Ternary nucleation involving ammonia and amines at atmospherically relevant concentrations enhances nucleation rates by a factor of 100–1000 according to the recent CLOUD experiment, but the extent of this enhancement is still being debated.[150,151] The same experiment found that ion-induced nucleation plays a sizable role. Ground level galactic cosmic rays generated ions that enhanced neutral nucleation rates by a factor of 2 at 298 K and more than 10 at 278 and 248 K.[1] Another possibility is the enhancing role of organic acids.[1,16,17] Still, binary, ternary, and ion-induced nucleation combined do not give nucleation rates as high as what has been observed in the atmosphere.

On the basis of the fundamental nucleation theorem, the power law dependence of the H_2SO_4–H_2O nucleation rate on H_2SO_4 concentration has been used to determine the number of H_2SO_4 molecules in the critical cluster. This number varies with $[H_2SO_4]$, RH, T, and type of nucleation mechanism, but what has been always found is that it is around 2 in atmospheric observations whereas lab measurements and theory suggest it should be a larger number. Some literature values at various $[H_2SO_4]$, RH, and T include 1–2,[7,11,17,21,152] 3–5,[1,23,151,153−155] 7–13,[13] and even a larger number of sulfuric acids.[5] Nevertheless, our work clearly demonstrates that the growth of single sulfuric acid hydrates is thermodynamically limited. In the absence of other species, further growth of this binary system toward a metastable critical nucleus at ambient

conditions will require high sulfuric acid concentration (10^9–10^{10}/cm^3). Yu[148] used classical binary homogeneous nucleation (CBHN)[49] theory to predict that at 217 K and ([H_2SO_4], RH) values of (10^9 cm^{-3}, 55%) and (10^7 cm^{-3}, 50%), the critical cluster contains about one sulfuric acid. However, at 273 K and ([H_2SO_4], RH) values of (10^9 cm^{-3}, 55%) and (10^7 cm^{-3}, 50%), the critical cluster contains 4 and 20 sulfuric acid molecules, respectively. Compared to CBHN, Yu's kinetic quasi-unary homogeneous nucleation theory (KQHN)[64] predicts slightly bigger critical clusters at lower temperatures and smaller ones at higher temperatures. In either case, the nucleation barrier to reach the critical cluster would be so large at conditions in the lower atmosphere ([H_2SO_4] ~ 10^7/cm^3, T > 273 K, RH < 100%) that binary H_2SO_4–H_2O nucleation cannot be a major source of new particles.

Using our Boltzmann-averaged Gibbs free energies, and various relative humidity values and temperatures, we found sulfuric acid's mono-, di-, and trihydrates to form in substantial numbers (Table 7) at equilibrium. With increasing RH, the equilibrium shifts toward the formation of hydrates over the unhydrated sulfuric acid, as shown in Figure 12. The combination of sulfuric acid monomers and/or hydrates to form dimers and bigger clusters is thermodynamically favorable,[156,157] but it might be kinetically limited because the number concentration of the sulfuric acid monomers and hydrates are much smaller than that of water monomers.[11] Using Gibbs free energies for the formation of sulfuric acid monomer and dimer hydrates, we found that the ratio of the number concentration of sulfuric acid dimer hydrates to monomer hydrates is about 10^{-3} at 216.15 K and 10^{-6} at 298.15 K, 100% RH and [H_2SO_4] = 5 × 10^7 cm^{-3} in an equilibrium situation. Perhaps BHN is a dominant source of new particles in combustion systems like coal-fired boilers, where the sulfuric acid vapor is formed in large numbers before the start of nucleation, or in colder regions of the troposphere where the nucleation barrier is low.[55] The progression of the nucleation mechanism from purely binary at 248 K to a mix of binary and ternary (with ammonia and amines) at 278 K to purely ternary at 292 K observed in the recent CLOUD experiment supports that idea.[1]

5. CONCLUSIONS

Using molecular dynamics configuration sampling with high-level quantum mechanical minimizations, we have determined many stable hydrates of sulfuric acid containing up to six waters. Our RI-MP2 binding energies have been extrapolated to the complete basis set limit and corrected for vibrational anharmonicity using scaling factors derived from VPT2 fundamental frequencies. Sulfuric acid hydrates [$H_2SO_4(H_2O)_n$] formed ionic pairs [$HSO_4^-H_3O^+(H_2O)_{n-1}$] upon the addition of four or more waters depending on the temperature. The calculated Gibbs free energies predict that the formation of $H_2SO_4(H_2O)_{n=1-6}$ is favorable in the colder regions of the troposphere (T = 216.65–273.15 K), but $H_2SO_4(H_2O)_{n>4}$ will not form in appreciable numbers at T = 298.15 K. Our calculated equilibrium hydrate distribution predicts that sulfuric acid does not form hydrates as overwhelmingly as predicted by other models and experiments. Rather, as much as 50–60% of the acid remains unhydrated at 20% RH and 10–15% at 100% RH in the troposphere. A proper treatment of hydrate formation can help decrease the discrepancy between theoretical and observed nucleation rates of sulfuric acid in the atmosphere. On the basis of the thermodynamics of $H_2SO_4(H_2O)_{n=1-6}$, it is unlikely that binary homogeneous nucleation contributes significantly to new particle formation at ambient conditions in the continental boundary layer. Perhaps in the colder regions of the troposphere, BHN can account for the observed nucleation rates. These predictions are consistent with the recent CLOUD experiment, which concluded that most new particle formation results from ternary nucleation at 278 and 292 K and binary nucleation at 248 K.[1]

■ ASSOCIATED CONTENT

Supporting Information

All the RI-MP2/aVDZ optimized geometries, a comparison of RI-MP2/aVTZ and RI-MP2/aVDZ geometries and binding energies, the effect of including an extra d-function of sulfur, a comparison of the RI-MP2 plain and extrapolated binding energies against benchmark DF-MP2-F12/VQZ-F12 values, Boltzmann averaged harmonic binding energies, VPT2/MP2/aVDZ anharmonic frequencies, the procedure for calculating scaling factors and ensemble averaging, and a comparison of CLD and RI-MP2/CBS hydration free energies. This information is available free of charge via the Internet at http://pubs.acs.org/.

■ AUTHOR INFORMATION

Corresponding Author

*E-mail: george.shields@bucknell.edu.

Notes

The authors declare no competing financial interest.

■ ACKNOWLEDGMENTS

Acknowledgment is made to the NSF and Bucknell University for their support of this work. This project was supported in part by NSF grant CHE-0848827, and by NSF grants CHE-0116435, CHE-0521063, and CHE-0849677 as part of the MERCURY high-performance computer consortium (http://www.mercuryconsortium.org). This research used the National Science Foundation TeraGrid resources provided by the Texas Advanced Computing Center (TACC) under grant number [TG-CHE090095]. This research also used resources of the National Energy Research Scientific Computing Center, which is supported by the Office of Science of the U.S. Department of Energy under Contract No. DE-AC02-05CH11231.

■ REFERENCES

(1) Kirkby, J.; Curtius, J.; Almeida, J.; Dunne, E.; Duplissy, J.; Ehrhart, S.; Franchin, A.; Gagne, S.; Ickes, L.; Kurten, A.; et al. *Nature* **2011**, *476*, 429–433.

(2) Foster, P.; Ramaswamy, V. In *Climate Change 2007 The Scientific Basis*; Solomon, S., Qin, D., Manning, M., Chen, Z., Marquis, M., Averyt, K. B., Tignor, M., Miller, H. L., Eds.; Cambridge University Press: Cambridge, U.K., 2007; p 137.

(3) Castleman, A. W. J. *Space Sci. Rev.* **1974**, *15*, 547–589.

(4) Kulmala, M.; Vehkamäki, H.; Petäjä, T.; Dal Maso, M.; Lauri, A.; Kerminen, V. M.; Birmili, W.; McMurry, P. H. *J. Aerosol Sci.* **2004**, *35*, 143–176.

(5) Seinfeld, J. H.; Pandis, S. N. *Atmospheric Chemistry and Physics: From Air Pollution to Climate Change*, 2nd ed.; John Wiley & Sons, Inc.: New York, 2006.

(6) Solomon, S.; Qin, D.; Manning, M. *Climate Change 2007: The Physical Science Basis*; Cambridge University Press: Cambridge, U.K. and New York, NY, 2007.

(7) Kulmala, M.; Lehtinen, K. E. J.; Laaksonen, A. *Atm. Chem. Phys.* **2006**, *6*, 787–793.

(8) Kulmala, M.; Riipinen, I.; Sipilä, M.; Manninen, H. E.; Petäjä, T.; Junninen, H.; Maso, M. D.; Mordas, G.; Mirme, A.; Vana, M.; et al. *Science* **2007**, *318*, 89−92.
(9) Weber, R. J.; Marti, J. J.; McMurry, P. H.; Eisele, F. L.; Tanner, D. J.; Jefferson, A. *J. Geophys. Res.* **1997**, *102*, 4375−4385.
(10) Kulmala, M.; Vehkamki, H.; Petäja, T.; Dal Maso, M.; Lauri, A.; Kerminen, V. M.; Birmili, W.; McMurry, P. H. *J. Aerosol Sci.* **2004**, *35*, 143−176.
(11) Kuang, C.; McMurry, P. H.; McCormick, A. V.; Eisele, F. L. *J. Geophys. Res.* **2008**, *113*, D10209.
(12) Kulmala, M.; Kerminen, V.-M. *Atmos. Res.* **2008**, *90*, 132−150.
(13) Ball, S. M.; Hanson, D. R.; Eisele, F. L.; McMurry, P. H. *J. Geophys. Res.* **1999**, *104*, 23709−23718.
(14) Kurtén, T.; Loukonen, V.; Vehkamäki, H.; Kulmala, M. *Atmos. Chem. Phys.* **2008**, *8*, 4095−4103.
(15) Loukonen, V.; Kurtén, T.; Ortega, I. K.; Vehkamäki, H.; Pádua, A. A. H.; Sellegri, K.; Kulmala, M. *Atm. Chem. Phys.* **2010**, *10*, 4961−4974.
(16) Zhang, R.; Suh, I.; Zhao, J.; Zhang, D.; Fortner, E. C.; Tie, X.; Molina, L. T.; Molina, M. J. *Science* **2004**, *304*, 1487−1490.
(17) Metzger, A.; Verheggen, B.; Dommen, J.; Duplissy, J.; Prevot, A. S. H.; Weingartner, E.; Riipinen, I.; Kulmala, M.; Spracklen, D. V.; Carslaw, K. S.; et al. *Proc. Natl. Acad. Sci.* **2010**, *107*, 6646−6651.
(18) Yu, F.; Turco, R. P. *Geophys. Res. Lett.* **2000**, *27*, 883−886.
(19) Curtius, J.; Lovejoy, E. R.; Froyd, K. D. *Space Sci. Rev.* **2006**, *125*, 159−167.
(20) Kerminen, V. M.; Petäjä, T.; Manninen, H. E.; Paasonen, P.; Nieminen, T.; Sipilä, M.; Junninen, H.; Ehn, M.; Gagné, S.; Laakso, L.; et al. *Atmos. Chem. Phys. Discuss.* **2010**, *10*, 16497−16549.
(21) Sipilä, M.; Berndt, T.; Petäjä, T.; Brus, D.; Vanhanen, J.; Stratmann, F.; Patokoski, J.; Mauldin, R. L.; Hyvarinen, A. P.; Lihavainen, H.; et al. *Science* **2010**, *327*, 1243−1246.
(22) Jiang, J.; Zhao, J.; Chen, M.; Eisele, F. L.; Scheckman, J.; Williams, B. J.; Kuang, C.; McMurry, P. H. *Aerosol Sci. Technol.* **2011**, *45*, ii−v.
(23) Berndt, T.; Boge, O.; Stratmann, F.; Heintzenberg, J.; Kulmala, M. *Science* **2005**, *307*, 698−700.
(24) Doyle, G. J. *J. Chem. Phys.* **1961**, *35*, 795−799.
(25) Kiang, C. S.; Stauffer, D. *Faraday Symp. Chem. Soc.* **1973**, *7*, 26−33.
(26) Mirabel, P.; Katz, J. L. *J. Chem. Phys.* **1974**, *60*, 1138−1144.
(27) Heist, R. H.; Reiss, H. *J. Chem. Phys.* **1974**, *61*, 573−581.
(28) Shugard, W. J.; Heist, R. H.; Reiss, H. *J. Chem. Phys.* **1974**, *61*, 5298−5304.
(29) Shugard, W. J.; Reiss, H. *J. Chem. Phys.* **1976**, *65*, 2827−2840.
(30) Marvin, D. C.; Shugard, W. J. *J. Chem. Phys.* **1977**, *67*, 5982−5982.
(31) Jaecker-Voirol, A.; Mirabel, P.; Reiss, H. *J. Chem. Phys.* **1987**, *87*, 4849−4852.
(32) Jaecker-Voirol, A.; Mirabel, P. *J. Phys. Chem.* **1988**, *92*, 3518−3521.
(33) Kulmala, M.; Laaksonen, A. *J. Chem. Phys.* **1990**, *93*, 696−701.
(34) Lazaridis, M.; Kulmala, M.; Laaksonen, A. *J. Aerosol Sci.* **1991**, *22*, 823−830.
(35) Laaksonen, A.; Kulmala, M. *J. Aerosol Sci.* **1991**, *22*, 779−787.
(36) Mirabel, P.; Ponche, J. L. *Chem. Phys. Lett.* **1991**, *183*, 21−24.
(37) Kulmala, M.; Lazaridis, M.; Laaksonen, A.; Vesala, T. *J. Chem. Phys.* **1991**, *94*, 7411−7413.
(38) Wyslouzil, B. E.; Seinfeld, J. H.; Flagan, R. C.; Okuyama, K. *J. Chem. Phys.* **1991**, *94*, 6842−6850.
(39) Kerminen, V. M.; Wexler, A. S. *Atmos. Environ.* **1994**, *28*, 2399−2406.
(40) Kulmala, M.; Kerminen, V. M.; Laaksonen, A. *Atmos. Environ.* **1995**, *29*, 377−382.
(41) Viisanen, Y.; Kulmala, M.; Laaksonen, A. *J. Chem. Phys.* **1997**, *107*, 920−926.
(42) Kusaka, I.; Wang, Z. G.; Seinfeld, J. H. *J. Chem. Phys.* **1998**, *108*, 6829−6848.
(43) Noppel, M. *J. Chem. Phys.* **1998**, *109*, 9052−9056.
(44) Pirjola, L.; Kulmala, M.; Wilck, M.; Bischoff, A.; Stratmann, F.; Otto, E. *J. Aerosol Sci* **1999**, *30*, 1079−1094.
(45) Noppel, M. *J. Geophys. Res.-Atmos.* **2000**, *105*, 19779−19785.
(46) Zaichik, L. I.; Lebedev, A. B.; Savel'ev, A. M.; Starik, A. M. *High Temp.* **2000**, *38*, 77−86.
(47) Laaksonen, A.; Pirjola, L.; Kulmala, M.; Wohlfrom, K. H.; Arnold, F.; Raes, F. *J. Geophys. Res.-Atmos.* **2000**, *105*, 1459−1469.
(48) Noppel, M.; Vehkamäki, H.; Kulmala, M. *J. Chem. Phys.* **2002**, *116*, 218−228.
(49) Vehkamäki, H.; Kulmala, M.; Napari, I.; Lehtinen, K. E. J.; Timmreck, C.; Noppel, M.; Laaksonen, A. *J. Geophys. Res.-Atmos.* **2002**, 107.
(50) Vehkamäki, H.; Kulmala, M.; Lehtinen, K. E. J.; Noppel, M. *Environ. Sci. Technol.* **2003**, *37*, 3392−3398.
(51) Hamill, P.; D'Auria, R.; Turco, R. P. *Annals Geophys.* **2003**, *46*, 331−340.
(52) Noppel, M. *Atmos. Res.* **2003**, *65*, 285−301.
(53) Yu, F. Q. *J. Chem. Phys.* **2005**, *122*, 074501.
(54) Yu, F. Q. *J. Geophys. Res.-Atmos.* **2006**, *111*, D03206.
(55) Bein, K. J.; Wexler, A. S. *J. Chem. Phys.* **2007**, 127.
(56) McGraw, R. *J. Chem. Phys.* **1995**, *102*, 2098−2108.
(57) Arstila, H. *J. Chem. Phys.* **1997**, *107*, 3196−3203.
(58) Sorokin, A.; Vancassel, X.; Mirabel, P. *J. Chem. Phys.* **2005**, *123*, 244508.
(59) Zhang, R.; Khalizov, A.; Wang, L.; Hu, M.; Xu, W. *Chem. Rev.* 2011.
(60) Marti, J. J.; Jefferson, A.; Cai, X. P.; Richert, C.; McMurry, P. H.; Eisele, F. *J. Geophys. Res.* **1997**, *102*, 3725−3735.
(61) McGraw, R.; Weber, R. J. *Geophys. Res. Lett.* **1998**, *25*, 3143−3146.
(62) Jaecker-Voirol, A.; Mirabel, P. *Atmos. Environ. (1967)* **1989**, *23*, 2053−2057.
(63) Hanson, D. R.; Eisele, F. *J. Phys. Chem. A* **2000**, *104*, 1715−1719.
(64) Yu, F. Q. *J. Chem. Phys.* **2007**, *127*, 054301.
(65) Arstila, H.; Laasonen, K.; Laaksonen, A. *J. Chem. Phys.* **1998**, *108*, 1031−1039.
(66) Bandy, A. R.; Ianni, J. C. *J. Phys. Chem. A* **1998**, *102*, 6533−6539.
(67) Re, S.; Osamura, Y.; Morokuma, K. *J. Phys. Chem. A* **1999**, *103*, 3535−3547.
(68) Ding, C. G.; Taskila, T.; Laasonen, K.; Laaksonen, A. *Chem. Phys.* **2003**, *287*, 7−19.
(69) Ding, C. G.; Laasonen, K. *Chem. Phys. Lett.* **2004**, *390*, 307−313.
(70) Al Natsheh, A.; Nadykto, A. B.; Mikkelsen, K. V.; Yu, F. Q.; Ruuskanen, J. *J. Phys. Chem. A* **2004**, *108*, 8914−8929.
(71) Nadykto, A. B.; Yu, F. In *Nucleation and Atmospheric Aerosols*; O'Dowd, C. D., Wagner, P. E., Eds.; Springer: Netherlands: 2007; p 297−301.
(72) Kurtén, T.; Torpo, L.; Ding, C. G.; Vehkamäki, H.; Sundberg, M. R.; Laasonen, K.; Kulmala, M. *J. Geophys. Res.* **2007**, *112*, D04210.
(73) Kurtén, T.; Sundberg, M. R.; Vehkamäki, H.; Noppel, M.; Blomqvist, J.; Kulmala, M. *J. Phys. Chem. A* **2006**, *110*, 7178−7188.
(74) Kurtén, T.; Noppel, M.; Vehkamäki, H.; Salonen, M.; Kulmala, M. *Boreal Environ. Res.* **2007**, *12*, 431−453.
(75) Jurema, M. W.; Shields, G. C. *J. Comput. Chem.* **1993**, *14*, 89−104.
(76) Jurema, M. W.; Kirschner, K. N.; Shields, G. C. *J. Comput. Chem.* **1993**, *14*, 1326−1332.
(77) Kirschner, K. N.; Shields, G. C. *Int. J. Quantum Chem.* **1994**, *28*, 349−360.
(78) Dunn, M. E.; Pokon, E. K.; Shields, G. C. *J. Am. Chem. Soc.* **2004**, *126*, 2647−2653.
(79) Dunn, M. E.; Pokon, E. K.; Shields, G. C. *Int. J. Quantum Chem.* **2004**, *100*, 1065−1070.
(80) Day, M. B.; Kirschner, K. N.; Shields, G. C. *Int. J. Quantum Chem.* **2005**, *102*, 565−572.
(81) Day, M. B.; Kirschner, K. N.; Shields, G. C. *J. Phys. Chem. A* **2005**, *109*, 6773−6778.

(82) Pickard, F. C.; Dunn, M. E.; Shields, G. C. *J. Phys. Chem. A* **2005**, *109*, 4905−4910.
(83) Pickard, F. C.; Pokon, E. K.; Liptak, M. D.; Shields, G. C. *J. Chem. Phys.* **2005**, *122*, 024302.
(84) Allodi, M. A.; Dunn, M. E.; Livada, J.; Kirschner, K. N.; Shields, G. C. *J. Phys. Chem. A* **2006**, *110*, 13283−13289.
(85) Alongi, K. S.; Dibble, T. S.; Shields, G. C.; Kirschner, K. N. *J. Phys. Chem. A* **2006**, *110*, 3686−3691.
(86) Dunn, M. E.; Evans, T. M.; Kirschner, K. N.; Shields, G. C. *J. Phys. Chem. A* **2006**, *110*, 303−309.
(87) Kirschner, K. N.; Hartt, G. M.; Evans, T. M.; Shields, G. C. *J. Chem. Phys.* **2007**, *126*, 154320.
(88) Allodi, M. A.; Kirschner, K. N.; Shields, G. C. *J. Phys. Chem. A* **2008**, *112*, 7064−7071.
(89) Dunn, M. E.; Shields, G. C.; Takahashi, K.; Skodje, R. T.; Vaida, V. *J. Phys. Chem. A* **2008**, *112*, 10226−10235.
(90) Hartt, G. M.; Shields, G. C.; Kirschner, K. N. *J. Phys. Chem. A* **2008**, *112*, 4490−4495.
(91) Shields, G. C.; Kirschner, K. N. *Synth. React. Inorg. Met.-Org. Chem.* **2008**, *38*, 32−36.
(92) Morrell, T. E.; Shields, G. C. *J. Phys. Chem. A* **2010**, *114*, 4266−4271.
(93) Shields, R. M.; Temelso, B.; Archer, K. A.; Morrell, T. E.; Shields, G. C. *J. Phys. Chem. A* **2010**, *114*, 11725−11737.
(94) Temelso, B.; Archer, K. A.; Shields, G. C. *J. Phys. Chem. A* **2011**, *115*, 12034−12046.
(95) Temelso, B.; Shields, G. C. *J. Chem. Theory Comput.* **2011**, *7*, 2804−2817.
(96) Case, D. A.; Darden, T.; Cheatham, T. E., III; Simmerling, C.; Wang, J.; Duke, R. E.; Luo, R.; Merz, K. M.; Pearlman, D. A.; Crowley, M. *AMBER 9*; University of California: San Francisco, 2006.
(97) Shaw, K. E.; Woods, C. J.; Mulholland, A. J. *J. Phys. Chem. Lett.* **2010**, *1*, 219−223.
(98) Wang, J.; Wolf, R. M.; Caldwell, J. W.; Kollman, P. A.; Case, D. A. *J. Comput. Chem.* **2004**, *25*, 1157−1174.
(99) Frisch, M. J.; Trucks, G. W.; Schlegel, H. B.; Scuseria, G. E.; Robb, M. A.; Cheeseman, J. R.; Montgomery, J. A.; Vreven, T.; Kudin, K. N.; Burant, J. C.;et al. *Gaussian 09*; Gaussian, Inc.: Wallingford, CT, 2009.
(100) Neese, F.; *ORCA 2.8.0*, 2.8.0 ed.; 2011.
(101) Feyereisen, M.; Fitzgerald, G.; Komornicki, A. *Chem. Phys. Lett.* **1993**, *208*, 359−363.
(102) Bernholdt, D. E.; Harrison, R. J. *Chem. Phys. Lett.* **1996**, *250*, 477−484.
(103) Dunning, T. *J. Chem. Phys.* **1989**, *90*, 1007−1023.
(104) Kendall, R.; Dunning, T.; Harrison, R. *J. Chem. Phys.* **1992**, *96*, 6796−6806.
(105) Woon, D.; Dunning, T. *J. Chem. Phys.* **1993**, *98*, 1358−1371.
(106) Weigend, F.; Kohn, A.; Hattig, C. *J. Chem. Phys.* **2002**, *116*, 3175−3183.
(107) Weigend, F.; Haser, M. *Theor. Chem. Acc.* **1997**, *97*, 331−340.
(108) Dunning, T. H.; Peterson, K. A.; Wilson, A. K. *J. Chem. Phys.* **2001**, *114*, 9244−9253.
(109) Klopper, W.; Bak, K. L.; Jorgensen, P.; Olsen, J.; Helgaker, T. *J. Phys. B-At. Mol. Opt. Phys.* **1999**, *32*, R103−R130.
(110) Boys, S. F.; Bernardi, F. *Mol. Phys.* **1970**, *19*, 533−566.
(111) Halkier, A.; Helgaker, T.; Jorgensen, P.; Klopper, W.; Koch, H.; Olsen, J.; Wilson, A. K. *Chem. Phys. Lett.* **1998**, *286*, 243−252.
(112) Halkier, A.; Helgaker, T.; Jorgensen, P.; Klopper, W.; Olsen, J. *Chem. Phys. Lett.* **1999**, *302*, 437−446.
(113) Klopper, W. *J. Chem. Phys.* **1995**, *102*, 6168−6179.
(114) Xantheas, S. S. *Philos. Mag. B* **1996**, *73*, 107−115.
(115) Xantheas, S. S. *J. Chem. Phys.* **1996**, *104*, 8821−8824.
(116) Xantheas, S. S.; Burnham, C. J.; Harrison, R. J. *J. Chem. Phys.* **2002**, *116*, 1493−1499.
(117) Xantheas, S. S.; Apra, E. *J. Chem. Phys.* **2004**, *120*, 823−828.
(118) Bryantsev, V. S.; Diallo, M. S.; van Duin, A. C. T.; Goddard, W. A. *J. Chem. Theory Comput.* **2009**, *5*, 1016−1026.
(119) Klopper, W.; Manby, F. R.; Ten-No, S.; Valeev, E. F. *Int. Rev. Phys. Chem.* **2006**, *25*, 427−468.
(120) Werner, H. J.; Knowles, P. J.; Knizia, G.; Manby, F. R.; Schuetz, M.; et al. *Molpro*; 2010.
(121) Werner, H. J.; Adler, T. B.; Manby, F. R. *J. Chem. Phys.* **2007**, *126*, 164102.
(122) Peterson, K. A.; Adler, T. B.; Werner, H. *J. Chem. Phys.* **2008**, *128*, 084102.
(123) Lane, J. R.; Kjaergaard, H. G. *J. Chem. Phys.* **2009**, *131*, 034307.
(124) Bischoff, F. A.; Wolfsegger, S.; Tew, D. P.; Klopper, W. *Mol. Phys.* **2009**, *107*, 963−975.
(125) Marshall, M. S.; Burns, L. A.; Sherrill, C. D. *J. Chem. Phys.* **2011**, *135*, 194102.
(126) Fanourgakis, G. S.; Apra, E.; Xantheas, S. S. *J. Chem. Phys.* **2004**, *121*, 2655−2663.
(127) Klopper, W.; Schutz, M.; Luthi, H. P.; Leutwyler, S. *J. Chem. Phys.* **1995**, *103*, 1085.
(128) Barone, V. *J. Chem. Phys.* **2004**, *120*, 3059−3065.
(129) Dunn, M. E.; Evans, T. M.; Kirschner, K. N.; Shields, G. C. *J. Phys. Chem. A* **2005**, *110*, 303−309.
(130) Pettersen, E. F.; Goddard, T. D.; Huang, C. C.; Couch, G. S.; Greenblatt, D. M.; Meng, E. C.; Ferrin, T. E. *J. Comput. Chem.* **2004**, *25*, 1605−1612.
(131) Kurtén, T. *Entropy* **2011**, *13*, 915−923.
(132) Curtiss, L. A.; Frurip, D. J.; Blander, M. *J. Chem. Phys.* **1979**, *71*, 2703−2711.
(133) Scribano, Y.; Goldman, N.; Saykally, R. J.; Leforestier, C. *J. Phys. Chem. A* **2006**, *110*, 5411−5419.
(134) Givan, A.; Larsen, L. A.; Loewenschuss, A.; Nielsen, C. J. *J. Mol. Struct.* **1999**, *509*, 35−47.
(135) Hintze, P. E.; Feierabend, K. J.; Havey, D. K.; Vaida, V. *Spectrochim. Acta A Mol. Biomol. Spectrosc.* **2005**, *61*, 559−566.
(136) Givan, A.; Larsen, L. A.; Loewenschuss, A.; Nielsen, C. J. *J. Chem. Soc., Faraday Trans.* **1998**, *94*, 827−835.
(137) Gerber, R. B.; Ratner, M. A. *Chem. Phys. Lett.* **1979**, *68*, 195.
(138) Miller, Y.; Chaban, G. M.; Gerber, R. B. *J. Phys. Chem. A* **2005**, *109*, 6565−6574.
(139) Truhlar, D. G.; Isaacson, A. D. *J. Chem. Phys.* **1991**, *94*, 357−359.
(140) Leopold, K. R. *Annu. Rev. Phys. Chem.* **2011**, *62*, 327−349.
(141) Rozenberg, M.; Loewenschuss, A. *J. Chem. Phys.* **2009**, *113*, 4963−4971.
(142) Kathmann, S. M.; Hale, B. N. *J. Phys. Chem. B* **2001**, *105*, 11719−11728.
(143) Sugawara, S.; Yoshikawa, T.; Takayanagi, T.; Shiga, M.; Tachikawa, M. *J. Phys. Chem. A* **2011**, *115*, 11486−11494.
(144) Ding, C. G.; Laasonen, K.; Laaksonen, A. *J. Phys. Chem. A* **2003**, *107*, 8648−8658.
(145) Grimme, S. *J. Comput. Chem.* **2004**, *25*, 1463−1473.
(146) Santra, B.; Michaelides, A.; Scheffler, M. *J. Chem. Phys.* **2007**, 127.
(147) Kathmann, S.; Schenter, G.; Garrett, B. *J. Phys. Chem. C* **2007**, *111*, 4977−4983.
(148) Yu, F. Q. *J. Geophys. Res.-Atmos.* **2008**, *113*, D24201.
(149) Kurtén, T.; Petäjä, T.; Smith, J.; Ortega, I. K.; Sipilä, M.; Junninen, H.; Ehn, M.; Vehkamäki, H.; Mauldin, L.; Worsnop, D. R.; et al. *Atmos. Chem. Phys.* **2011**, *11*, 3007−3019.
(150) Erupe, M. E.; Viggiano, A. A.; Lee, S. H. *Atmos. Chem. Phys.* **2011**, *11*, 4767−4775.
(151) Benson, D. R.; Yu, J. H.; Markovich, A.; Lee, S. H. *Atmos. Chem. Phys.* **2011**, *11*, 4755−4766.
(152) Hanson, D. R.; Eisele, F. L. *J. Geophys. Res.* **2002**, *107*, 4158.
(153) Eisele, F. L.; Hanson, D. R. *J. Phys. Chem. A* **2000**, *104*, 830−836.
(154) Nadykto, A. B.; Yu, F.; Herb, J. *Int. J. Mol. Sci.* **2008**, *9*, 2184−2193.
(155) Zhao, J.; Eisele, F. L.; Titcombe, M.; Kuang, C.; McMurry, P. H. *J. Geophys. Res.* **2010**, *115*, D08205.

(156) Hanson, D. R.; Lovejoy, E. *J. Phys. Chem. A* **2006**, *110*, 9525−9528.
(157) Petäjä, T.; Sipilä, M.; Paasonen, P.; Nieminen, T.; Kurtén, T.; Ortega, I. K.; Stratmann, F.; Vehkamäki, H.; Berndt, T.; Kulmala, M. *Phys. Rev. Lett.* **2011**, *106*, 228302.